Hydration and dehydration at the tropical tropopause

Cornelius Schiller

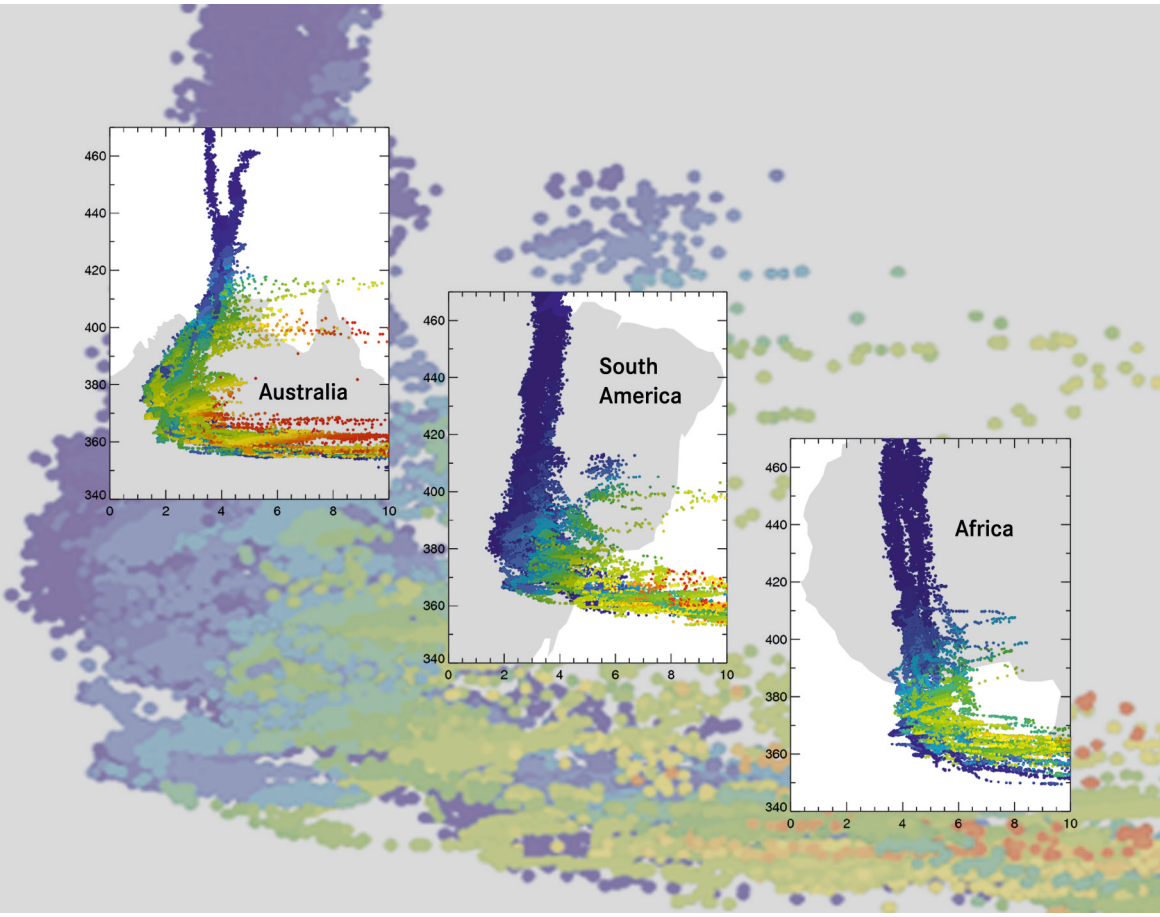

Energie & Umwelt / Energy & Environment
Band / Volume 295
ISBN 978-3-95806-101-9

JÜLICH FORSCHUNGSZENTRUM

Member of the Helmholtz Association

Schriften des Forschungszentrums Jülich
Reihe Energie & Umwelt / Energy & Environment Band / Volume 295

Forschungszentrum Jülich GmbH
Institute of Energy and Climate Research
Stratosphere (IEK-7)

Hydration and dehydration at the tropical tropopause

Cornelius Schiller

Schriften des Forschungszentrums Jülich
Reihe Energie & Umwelt / Energy & Environment Band / Volume 295

ISSN 1866-1793 ISBN 978-3-95806-101-9

Bibliographic information published by the Deutsche Nationalbibliothek.
The Deutsche Nationalbibliothek lists this publication in the Deutsche Nationalbibliografie; detailed bibliographic data are available in the Internet at http://dnb.d-nb.de.

Publisher and Distributor: Forschungszentrum Jülich GmbH
Zentralbibliothek
52425 Jülich
Tel: +49 2461 61-5368
Fax: +49 2461 61-6103
Email: zb-publikation@fz-juelich.de
www.fz-juelich.de/zb

Cover Design: Grafische Medien, Forschungszentrum Jülich GmbH

Printer: Grafische Medien, Forschungszentrum Jülich GmbH

Copyright: Forschungszentrum Jülich 2015

Schriften des Forschungszentrums Jülich
Reihe Energie & Umwelt / Energy & Environment, Band / Volume 295

468 (Habil.-Schr., Wuppertal, Univ., 2011)

ISSN 1866-1793
ISBN 978-3-95806-101-9

The complete volume is freely available on the Internet on the Jülicher Open Access Server (JuSER) at www.fz-juelich.de/zb/openaccess.

Neither this book nor any part of it may be reproduced or transmitted in any form or by any means, electronic or mechanical, including photocopying, microfilming, and recording, or by any information storage and retrieval system, without permission in writing from the publisher.

Preface

This book constitutes the habilitation thesis ("Habilitationsschrift") of Dr. Cornelius Schiller, which was accepted on 21 December 2011 by the "Habilitationskommission" of the Bergische Universität Wuppertal under the direction of Prof. Dr. Klümper. After the acceptance of the habilitation thesis, the process of habilitation at the Bergische Universität Wuppertal requires a lecture on a topic outside of the applicants subject area. The habilitation is finally awarded after a public lecture ("Antrittsvorlesung"), after which also the "venia legendi" is bestowed.

Because of his illness, Cornelius Schiller was not able to give the required lectures and therefore could not complete the habilitation process. He passed away on 3 March 2012.

The habilitation thesis of Cornelius Schiller is a cumulative thesis, i.e. it is based on research published in a series of articles in scientific journals. The original thesis contained reprints of these articles, while this book contains the abstracts. The book further contains an obituary for Cornelius Schiller, originally published in the journal EOS[1].

Through this book, we would like to make the habilitation thesis of Cornelius Schiller available to the public. We hope that it will not only serve to hold up the memory for Cornelius Schiller and his scientific work, but will also be a useful resource for those who, like himself, engage in research on water vapour and clouds in the atmosphere and their implications for climate.

Martina Krämer, Rolf Müller, Martin Riese, and Fred Stroh

[1] EOS, vol. 93, no. 32, p. 311, 2012. Copyright AGU. Reproduced by permission.

G E O P H Y S I C I S T S

Cornelius Schiller (1961–2012)

PAGE 311

Cornelius Schiller, an international leader in high-altitude water vapor measurements and quality assessment who took charge of several research campaigns and mentored many young scientists, passed away on 3 March 2012 in Neuss, Germany, after a battle with cancer. He was 50 years old.

Cornelius spent his childhood and most of his life in the Niederrhein region of Germany, close to Düsseldorf. He studied physics at the University of Bonn, and his developing interest in the physics and chemistry of the atmosphere led him to work with Dieter Ehhalt at the Forschungszentrum Jülich (Research Centre Jülich) in Germany. Cornelius' career started shortly after the discovery of the ozone hole, and he had the opportunity to participate in the first large-scale ozone measurement campaign in the Arctic, known as the Airborne Arctic Stratospheric Expedition, during January and February 1989; he contributed airborne observations of ozone-depleting chlorine and bromine substances.

Throughout most of his career, Cornelius's scientific interests focused on making and analyzing highly precise water vapor measurements in the upper troposphere and stratosphere (UT/S). In the mid 1990s, he established the water vapor group in the stratospheric research program at the Jülich research center. He led this group for the past 20 years.

Cornelius developed the Fast In situ Stratospheric Hygrometer (FISH), which has served as a reference for UT/S water measurements on balloons and aircraft worldwide for more than a decade now. A hygrometer (from the ancient Greek words *hygrós* (humid) and *métron* (measure)) is an instrument that determines the humidity of air. FISH uses the Lyman-α photofragment fluorescence technique to measure water vapor, and unlike standard operational hygrometers, it is accurate at the very low concentrations present in UT/S. With the development of FISH, Cornelius started a new era in measuring water vapor in the upper troposphere and lower stratosphere. Taking quality water vapor measurements under the conditions in this altitude region of the atmosphere is exceedingly difficult, but Cornelius and his Jülich colleagues succeeded in pushing the boundaries of science and technology by taking measurements with FISH on multiple platforms and at various latitudes from the deep tropics to the high Arctic. Thanks to Cornelius's sense that assessing the absolute accuracy of measurements at UT/S water is extremely important, FISH has been at the forefront of international efforts to study UT/S water vapor.

Cornelius served as lead author and coinitiator of Stratospheric Processes and Their Role in Climate assessments of stratospheric water vapor. He also played important roles in large-scale European and U.S. projects related to the stratosphere and its interaction with climate (e.g., Stratosphere Troposphere Experiment by Aircraft Measurements; the Third European Stratospheric Experiment on Ozone; the European Polar Stratospheric Cloud and Lee Wave Experiment; the Tropical Convection, Cirrus, and Nitrogen Oxides Experiment; Stratospheric-Climate Links with Emphasis on the Upper Troposphere and Lower Stratosphere (SCOUT-O3); African Monsoon Multidisciplinary Analyses-SCOUT-O3; and NASA's Mid-latitude Airborne Cirrus Properties Experiment (MACPEX)).

One of Cornelius's major achievements was his contribution in establishing the Russian-owned high-altitude research airplane Geophysica as part of the European research infrastructure. In 2005, within the SCOUT-O3 project, he managed the extraordinary task of facilitating Geophysica's flight to Australia; with landings in India, Indonesia, and Thailand and with diplomatic permissions to take measurements along the entire route. Because of his dedication to Geophysica, this unique research platform is expected to remain available to the European research community for the foreseeable future.

Up until his untimely death, Cornelius continued to work in his signature disciplined, well-organized manner. In spring 2011, while undergoing chemotherapy treatment, Cornelius participated in the MACPEX airborne field campaign in Houston, Tex., to investigate cirrus cloud properties and processes that affect radiation. He managed to do what not many non-U.S. scientists had done: flew "his" instrument, the FISH, on a NASA high-altitude WB-57 aircraft to contribute to the comparison of a number of U.S. hygrometers. While in cancer treatment, Cornelius also finished the thesis for his habilitation, the highest academic qualification a scholar can achieve at a German university, and played a central role in coordinating a new research proposal involving a Geophysica campaign.

Cornelius Schiller

Cornelius was not only an excellent, focused, and hard-working scientist but also a friendly, modest, and encouraging person of integrity who was highly respected among his peers. He was also an important mentor for the next generation of young scientists. The motivation for his work was always clear: He strived for scientific truth and obtaining a better understanding of Earth's atmosphere and climate. He was inspired by the need for environmental protection and the quest to safeguard the Earth for future generations.

He also had a delightful sense of humor and a strong loyalty to his home region, where he spent most of his life. He enjoyed attending the famous carnival in Düsseldorf, supported local traditions as a member of a Schützenverein (marksmen club) in Neuss, and was an enthusiastic supporter of the Fortuna Düsseldorf football team. He was active in his church and served as the head of his local parish council. Above all, Cornelius was devoted to his family, including his wife, Barbara, and his children, Katharina, Andreas, and Christoph.

Cornelius left us behind all too early. He had many plans and was still actively working on his initiative for improved water vapor measurements. We will not forget him and will continue to work in his spirit on the questions that he raised about the processes controlling water vapor in UT/S and their impact on the Earth's climate.

—Karen Rosenlof, Earth System Research Laboratory, National Oceanic and Atmospheric Administration, Boulder, Colo.; and Rolf Müller, Forschungszentrum Jülich, Institute of Energy and Climate Research, Jülich, Germany; E-mail: ro.mueller@fz-juelich.de

© 2012. American Geophysical Union. All Rights Reserved.

Hydration and dehydration at the tropical tropopause

Habilitationsschrift zur Erlangung der venia legendi
im Fachbereich C – Mathematik und Naturwissenschaften, Fachgruppe Physik
der Bergischen Universität Wuppertal

Cornelius Schiller

Institut für Energie- und Klimaforschung 7: Stratosphäre
Forschungszentrum Jülich GmbH

März 2011

Für Barbara, Katharina, Andreas und Christoph

Alles ist aus dem Wasser entsprungen!
Alles wird durch das Wasser erhalten!

The principle of all things is water.
All things are retained by water.

Thales of Miletus (624-546 BC) in 'Faust. Der Tragödie zweiter Teil' by J. W. Goethe (1832)

Content

Abstract

Changes of stratospheric water budget are connected to the water entry which is set by the cold trap at the tropical tropopause. Airborne measurement of water over the Indian Ocean, Brazil, Australia and Burkina Faso are used to investigate, along which pathways air is freeze-dried on its way into the stratosphere and which conditions control the freeze-drying processes. The results critically depend on the accuracy of the data set which is compared to that of other scientists in field and laboratory experiments. The tropical water entry is a highly complex interplay between freeze-drying in the coldest regions of the tropical tropopause layer and fresh supply of water by convection or by mixing with tropospheric air. Trajectory-based reconstruction of water yields a remarkable agreement with the observations and proofs the concept that stratospheric water entry is primarily controlled by the coldest regions in the tropics. The net effect of deep convection is moistening, locally also above the tropopause. However, no indication of a global convective impact on the stratospheric water budget can be derived. Thus large-scale transport is dominant compared to that by convection. Cirrus clouds are a key parameter in the freeze-drying process, and their ice water content is an indication on their hydration or dehydration potential. The cloud formation critically depends on the relative humidity. In contrast to some recent studies, the data set here confirms the atmospheric distribution of saturation in agreement with accepted theories. The observed moderate supersaturations have only a limited impact on the water entry.

Kurzfassung

Änderungen des stratosphärischen Wasserbudgets sind an den Wassereintrag über die Kühlfalle an der tropischen Tropopause gekoppelt. Hier werden Flugzeugmessungen von Wasser über dem Indischen Ozean, Brasilien, Australien und Burkina Faso genutzt, um zu untersuchen, entlang welcher Pfade Luft auf dem Weg in die Stratosphäre gefriergetrocknet wird und welche Bedingungen die Trocknungsprozesse bestimmen. Die Ergebnisse hängen empfindlich von der Genauigkeit des Datensatzes ab, der in Labor- und Feldexperimenten mit denen anderer Wissenschaftler verglichen wird. Der tropische Wassereintrag ist ein komplexes Zusammenspiel zwischen Gefriertrocknung in den kältesten Regionen der tropischen Tropopausenschicht und Nachschub von Wasser durch Konvektion oder durch Mischung mit troposphärischer Luft. Trajektoriengestützte Rekonstruktion von Wasser zeigt eine sehr gute Übereinstimmung mit den Messungen und ist ein Beweis für die Hypothese, dass der stratosphärische Wassereintrag vornehmlich durch die kältesten Regionen der Tropen bestimmt wird. Hochreichende Konvektion führt netto zu einer Befeuchtung, die lokal auch über die Tropopause reichen kann. Allerdings lässt sich kein globaler konvektiver Einfluss auf das Wasserbudget ableiten. Daher spielt großskaliger Transport gegenüber Konvektion eine übergeordnete Rolle. Zirruswolken sind der Schlüssel für die Trocknungsprozesse, und deren Eiswassergehalt ist ein Indikator für deren Hydratations- bzw. Dehydratationspotential. Die Wolkenbildung wird besonders durch die relative Feuchte bestimmt. Anders als einige kürzlich erschienene Studien ergibt der hier vorgestellte Datensatz eine Verteilung der Sättigung in der Atmosphäre, der gängige Theorien bestätigt. Die beobachteten moderaten Übersättigungen besitzen nur einen begrenzten Einfluss auf den Wassereintrag.

1 Introduction

1.1 Changes of stratospheric water concentrations

The concentration of water vapour in the stratosphere is changing. In the 1980ies and 1990ies, the observed increase reached a magnitude of 1% per year (Kley et al., 2000; Rosenlof et al., 2001); this number was revised in a more recent analysis to 0.7% per year for this period (Scherer et al., 2008), but still results in a remarkable augmentation of water over these decades. Then in 2000, an unexpected sudden drop by about 10% was observed (e.g. Randel et al., 2006), accompanied by an abrupt decrease in temperatures at the tropical tropopause in that year. And in recent years, stratospheric water concentrations seem to increase again (Jones et al., 2009; Hurst et al., 2011).

The consequences of a changing water budget in stratosphere are manifold, as water is the most important greenhouse gas, as it controls nucleation of clouds and as it is a precursor of reactive chemistry involving the OH radical: Though less than 1% of atmospheric water content is found in the stratosphere, it impacts the Earth's radiation budget significantly and received attention in the IPCC 2007 report. Forster and Shine (1999) calculated that the increase of stratospheric water resulted in an additional global warming thus alarming the community; this finally results in the SPARC initiative (SPARC = Stratospheric Processes and their Role in Climate is a programme of the World Climate Research Programme, WCRP) towards the Water Vapour Assessment in 2000 (Kley et al., 2000). Today, Solomon et al. (2010) argue that the rate of surface warming was enhanced by 30% due to the increase by stratospheric water in that period, while it slowed down in the last decade by about 25% due to the drop afterwards.

Changing water concentrations, together with changing temperatures, also impact the ability to form clouds as described by the Clausius Clapeyron equation. In the stratosphere, an increase of water results in a higher frequency of polar stratospheric clouds (PSC), which by themselves provide a surface for heterogeneous conversion of halogen species in ozone destroying substances. As the formation of clouds depends on a threshold condition of temperature and water concentration, even small changes might result in a large change of cloud occurrence frequency, in particular in the Arctic polar stratosphere. Thus an increase in stratospheric water likely results in larger ozone destruction or at least delays the beginning recovery of the ozone layer (Dvortsov and Solomon, 2001; Feck et al., 2008).

In the stratosphere, the mixing ratios of water and methane are tightly coupled, as oxidation of each molecule of CH_4 produces approximately two molecules of H_2O (e.g. LeTexier et al., 1988). An obvious reason for an increase of stratospheric water is therefore the atmospheric concentration increase of its source gas methane. However, based on balloon-borne observations of CH_4 we calculated that only 30% of the observed water increase in the 1980ies and 1990ies is due to the increasing methane concentrations (Rohs et al., 2006). Though the atmospheric increase of CH_4 has slowed down in the last years (Dlugokencky et al., 2003), this phenomenon cannot account for the sudden drop of stratospheric H_2O in 2000.

Beside methane oxidation, stratospheric water has its origin from direct transport from the troposphere; in Engel et al. (1996), we derived from CH_4 and H_2O measurements an average

entry value of 3.6 ppmv. Air enters the stratosphere in the tropics and feeds the middle atmosphere with natural and anthropogenic substances. For water, the tropical tropopause plays a special role, as it acts as a cold trap: The very low temperatures at these altitudes freeze-dry the rising air to very low mixing ratios of typically only a few ppmv, the resulting ice particles sediment-out and remove the excess water from the air entering the stratosphere. Therefore, processes in the so-called tropical tropopause layer (TTL) are the key to understand changes of stratospheric water on all time scales. From these principles, two fundamental questions need to be answered:

Along which pathways is water transported and freeze-dried on its way into the stratosphere? Which conditions do control the freeze-drying process at the tropical tropopause?

1.2 Water transport across the tropical tropopause

The entry of water vapour into the stratosphere is controlled by the interplay of transport and freeze-drying primarily in the tropics (e.g. Fueglistaler et al., 2009, and references therein). Several hypotheses have been proposed to explain the dryness of the stratosphere and the variability of the water entry. The average temperature and corresponding saturation ice mixing ratio at the tropical tropopause are higher than the observed average water entry would require. Therefore, Newell and Gould-Stewart (1981) proposed fountain regions where the entry into the stratosphere is preferred and where tropopause temperatures are coldest, as the region of the Western Pacific during the northern hemispheric winter and the Bay of Bengal during northern hemispheric summer. Taking up the idea of dedicated regions of effective freeze-drying, Holton and Gettelman (2001) proposed that horizontal advection through these cold tropopause regions is causing the dryness of air before entering the stratosphere, rather than enhanced upwelling in these particular regions. Several climatological studies based on a Lagrangian approach (e.g. Jensen and Pfister, 2004; Fueglistaler et al., 2005; Fueglistaler and Haynes, 2005) demonstrated that saturation mixing ratios along trajectories provide a good first-order estimate for stratospheric water vapour mixing ratios and their variability on seasonal and interannual scales. Such studies of large-scale dehydration confirm the important role of the Western Pacific and the Asian monsoon regions to control the moisture flux into the stratosphere.

As an alternative hypothesis to large-scale dehydration, Danielsen (1993) and Sherwood and Dessler (2000) postulated that dehydration occurs primarily in deep overshooting convection. Extremely low temperatures in cumulonimbus turrets may lead to extremely dry air, providing that the air is exposed to lowest temperatures for a sufficiently long time to allow for the ice particles to sediment-out. However, more recent studies (Chaboureau et al., 2007; Grosvenor et al., 2007; Jensen et al., 2007) imply that overshooting convection has rather a hydrating than dehydrating effect close to the tropical tropopause. Upscaling of overshoot events still reveals a large uncertainty for the estimation of their global impact on the stratospheric water budget.

1.3 Freeze-drying at the tropical tropopause

The formation of ice clouds in the tropical tropopause layer and their subsequent sedimentation is the process which determines the dryness of air entering the stratosphere. The key parameter controlling the formation of cirrus clouds is the relative humidity over ice RH_{ice}. Prior to ice formation, when an air parcel cools while rising, RH_{ice} increases up to the freezing threshold necessary to nucleate ice. This freezing threshold depends on the compounds of the available ice forming aerosols. If these aerosol particles are pure liquid solutions, homogeneous freezing occurs with temperature-dependent thresholds ranging from 140 to 180 % (Koop et al., 2000). In the presence of insoluble aerosol particles, the particles freeze heterogeneously with lower thresholds determined by the composition of the aerosol.

In the past, measurements of RH_{ice} inside and outside clouds gave sometimes surprising results, which seem to contradict the current understanding of cloud formation (Peter et al., 2006, and references therein): In several cases, clear sky observations show RH_{ice} above the homogeneous freezing threshold, occasionally even exceeding water saturation (e.g. Jensen et al., 2005). And the frequent in-cloud measurement of RH_{ice} exceeding 100% (e.g. Gao et al., 2004) also raised the question of freezing suppressing processes not known so far. Though several new theoretical and laboratory investigations were made since then to explain the striking observations, another question is discussed recently: How reliable are these measurements, often made at the limits of the instruments, and are such observations really robust in all data sets?

The question on new nucleation theories on the one side and the reliability of water measurements at low mixing ratios on the other side is crucial if we want to determine, at which thresholds ice cloud formation occurs, which number densities and thus size of the ice particles can be reached in ice clouds, and subsequently, how effective air is freeze-dried, in particular under the very cold conditions at the tropical tropopause.

1.4 Scope of this work

This work is based on a comprehensive data set of high-resolution measurements of atmospheric water which my research group obtained in the last decade from four field experiments in the tropics. This measurement programme was planned in response to the SPARC 2000 Water Vapour Assessment (Kley et al., 2000) to investigate key processes controlling the stratospheric water vapour entry across the tropical tropopause. An overview on the various campaigns, of which I myself organised and coordinated the SCOUT-O3 Darwin campaign (Vaughan et al., 2009), is given in Chapter 3.

Chapter 2 describes the hygrometer (Zöger et al., 1999; Meyer et al., 2011) which we developed in my research group at the Forschungszentrum Jülich and deployed in more than 20 field campaigns during the last two decades. Special emphasise is lead on the quality characteristics of this instrument and the data sets, following the problems addressed in Section 1.3. This includes the intercomparison with hygrometers of other groups, including a recent comprehensive laboratory experiment involving the world-leading hygrometers.

In Chapter 4, I present results of the four tropical campaigns and discuss these data in the light of various transport path ways through the TTL, i.e. large scale advection combined with slow rising and fast uplift in deep convective systems. The work is primarily based on four publications, of which Schiller et al. (2009) is the central one summarising and comparing the results of all campaigns (with a focus on the three most recent ones); this manuscript also includes trajectory modelling for the interpretation of the data. In Corti et al. (2008) we discuss the role of convection as observed from the Darwin experiment, while in MacKenzie et al. (2006) we describe the findings of our Indian Ocean experiment. The Chapter gives also an outline on various modelling studies in which our data have been used and which complement our key publications. E.g. Konopka et al. (2007) describes processes at the edge of the tropics and mixing with mid-latitude air from the Brazilian mission leading to new concepts of transport in the TTL.

In Chapter 5, I summarise our findings concerning ice clouds and saturation. A highlight is that our tropical measurements allow investigations down to the lowest temperatures of 185 K and low water mixing ratios of only 1-2 ppmv, where nucleation processes are different from the warmer conditions at the extratropical tropopause. First, the ice water content of cirrus clouds is investigated in a climatological study (Schiller et al., 2008a). This work is complemented by a description of the thinnest clouds ever observed (Luo et al., 2003a), based on our Indian Ocean data. In Krämer et al. (2009), we analyse our saturation data inside and outside of clouds: After a consequent quality control described in Chapter 2, our data do not confirm the striking result of other research groups, they rather provide evidence for our canonical understanding of ice nucleation but with some new aspects.

In my Conclusions (Chapter 6), I will try a first assessment of the new findings in the context of questions arising from the SPARC 2000 Water Vapour Assessment and the supersaturation discussion stimulated by Peter et al. (2006). As an outlook, a new SPARC Assessment is planned to be compiled soon, addressing these topics together with a continuation of the water trend assessment; an outline and the rational of the SPARC initiative towards a new Assessment is given in Schiller et al. (2008b).

The key publications cited in this outline are re-printed in the Appendix for more detailed information than I summarise in the individual Chapters.

2 Measurement of water in the upper troposphere and lower stratosphere

2.1 The Fast In-situ Stratospheric Hygrometer

The data set used in this work is measured by means of the Fast In-Situ Stratospheric Hygrometer (FISH) developed at the Forschungszentrum Jülich (Zöger, 1996; Zöger et al., 1999). The instrument is based on the Lyman-α photofragment fluorescence technique developed in the 1970ies e.g. by Kley and Stone (1978). H_2O molecules in the measurement cell are dissociated by radiation at wavelengths $\lambda < 137$ nm

$$H_2O + hv\ (\lambda < 137\ nm) \rightarrow OH^* + H \quad (1)$$

The produced electronically excited radical OH* relaxes to the ground state by fluorescence

$$OH^* \rightarrow OH + hv\ (\lambda = 305\text{-}325\ nm) \quad (2)$$

By measuring the fluorescence radiation at λ = 305-325 nm, the H_2O abundance is determined. The signal is – due to the competing collision of OH* with air molecules – a measure of the H_2O mixing ratio for ambient pressures higher than 30 hPa (Kley and Stone, 1978). Therefore, this method is especially suited for measurements in the upper troposphere and lower stratosphere (UTLS), where large gradients of the mixing ratios occur while the pressure gradients can be neglected. FISH is sensitive to measure mixing ratios from 1 – 1000 ppmv which is the relevant range for measurements in the UTLS.

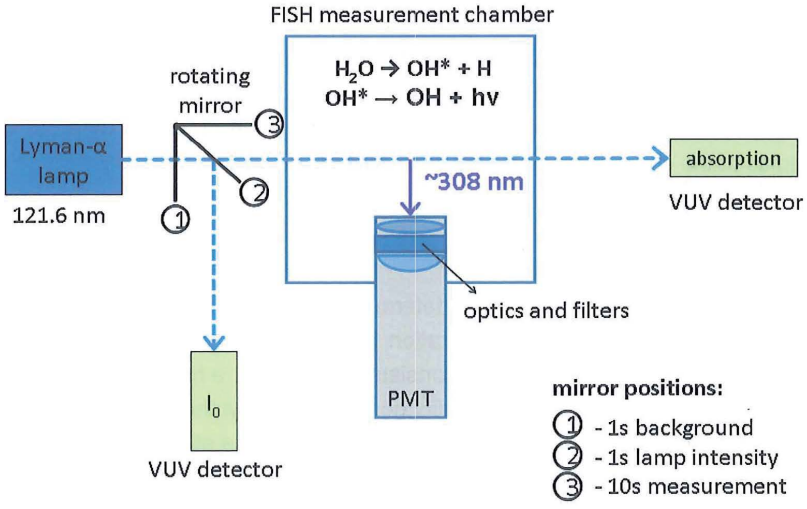

Figure 1: *Scetch of the FISH fluorescence cell and major optical components.*

The FISH design is schematically shown in Figure 1. It consists basically of the closed measurement cell, a Lyman-α radiation source, a photomultiplier tube to detect the fluorescence radiation and a detector to monitor the Lyman-α intensity of the lamp. A revolving mirror switches between the different modes determining a measurement cycle. The H_2O mixing ratio μ is determined from the total fluorescence counts N_g (mirror in position 1) from which

the background counts N_u (mirror in position 3) have to be subtracted and divided by the lamp intensity I_0:

$$\mu = c_k \cdot (N_g - f_u \cdot N_u) / I_0 \quad (3)$$

Hereby, c_k and f_u are factors which are determined in the calibration procedure described in Section 2.2.

So far, we designed five different FISH instruments for the use on balloon and various research aircraft. Here, we report data obtained from the Russian high altitude aircraft M55 Geophysica with a ceiling up to 20 km altitude (50 hPa). Flow rates through the cell are maintained, even at the lowest pressure of 50 hPa, to 5 standard litres per minute in order to minimize potential surface contamination effects. The flow rate also limits the time resolution of the cell in which the air is exchanged, i.e. typically within 1 s.

The inlet of FISH onboard the Geophysica aircraft is a heated, forward facing tube to sample total water, i.e. the sum of gas phase water and water bound in particles, which evaporate in the inlet tube before measured in the cell. Particles are sampled with enhanced efficiency compared to water vapour molecules; the so-called enhancement factor for particle sampling is determined from computational fluid-dynamic calculations of the inlet for different flight conditions and the relevant particle size spectrum (Krämer and Afchine, 2004). For measurements in clouds, the particle contribution of the total water measurement needs to be corrected by this enhancement factor as described in Schiller et al. (2008a) and in Chapter 5.

Complementary to the total water measurements of FISH, another Lyman-α fluorescence hygrometer is flown onboard the Geophysica, the FLuorescent Airborne Stratospheric Hygrometer (FLASH) instrument operated by the Russian CAO group (Sitnikov et al., 2007). The inlet of FLASH is designed to measure gas-phase water only, so the combination of both instruments provides distinct information for measurements in clouds. The FLASH data set is used in the quality discussion in Section 2.3 in comparison with our FISH data set and for scientific studies of the cloud measurements in Chapter 5.

2.2 Calibration of FISH

FISH is regularly calibrated in the laboratory determining the coefficients c_k and f_u in Equation (3). For this purpose, we developed a calibration bench which is described in Zöger et al. (1999) and Meyer et al. (2011). The device consists of two parts, a humidity generator and a reference hygrometer (Figure 2). In the humidity generator, dry synthetic air is moistened in a thermo-stabilised bubbler, typically generating mixing ratios in the air from less than 1 ppmv to 1000 ppmv. This air stream is divided to FISH, where pressures can be varied between 1000 and 10 hPa, and the reference hygrometer. Thus, a calibration can be carried out for the relevant conditions expected for measurements in the UTLS.

The reference instrument is a commercial frost point hygrometer. Until 2001 we used a General Eastern model 1311DRX and since then a MBW model K-1806/DP30 (hereafter denoted as DP30). The following accuracy discussion is based on the DP30 hygrometer. The earlier measurements using calibrations the General Eastern hygrometer likely have lower accuracy

than those stated below, e.g. data obtained during the APE-THESEO 1999 campaign which amongst others are used in this work.

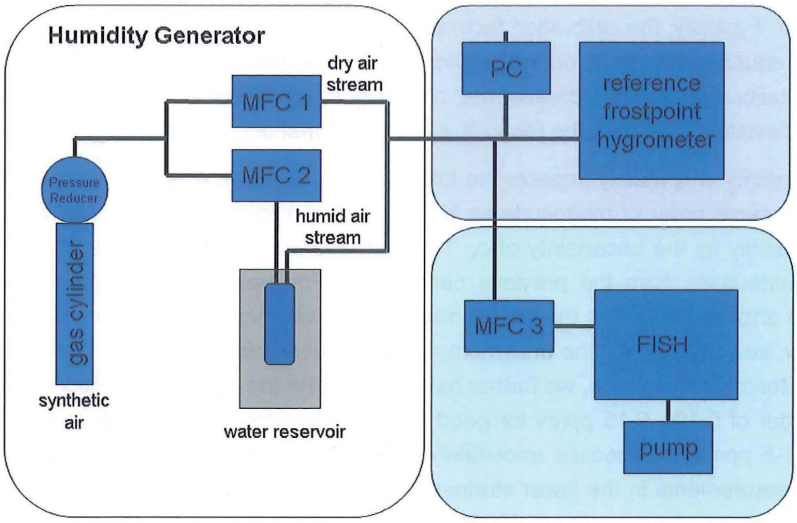

Figure 2: *Sketch of the calibration bench for FISH*

The accuracy of the DP30 reference is tested by three independent methods (Meyer, 2008; Meyer et al., 2011). The instrument is calibrated by the manufacturer against a reference instrument traceable to the UK primary standard at the National Physical Laboratory (NPL). This calibration was repeated in 2007 with negligible differences to the original calibration six years before. Further, as we deploy two DP30 instruments, we regularly check their differences which are on the order of 0.1-0.2 K in frost point. So we can demonstrate the self consistency and long-term stability of our reference hygrometers. An independent check of the absolute accuracy is the comparison against a permeation source, a secondary standard of the German Physikalisch-Technische Bundesanstalt (PTB) in 2008. The deviations from this PTB standard were lower than ± 2%. Hereby, we also checked the sensitivity on different conversion functions between frost point temperature and concentration, which are summarised in Murphy and Koop (2005): the function of Sonntag (1994) which is used by default in the DP30 conversions results in a maximum deviation of ± 1% from the mean value of all equations. In summary, an accuracy of the DP30 reference of 2-3% in mixing ratio is confirmed by seveal independent comparisons traceable to independent national standards.

In calibration runs with an extended pressure and mixing ratio range, we found that Equation (3) can only be applied with pressure-dependent calibration factors c_k and f_u (Meyer et al., 2011). For the range of mixing ratios and pressures which are relevant for our UTLS studies, however, we can determine constant factors c_k and f_u which simplifies the data retrieval. The error arising from the use of 'mean' or 'optimised' calibration factors is typically 2-4% for c_k and 10-15% for f_u for relevant conditions in the UTLS. But during the laboratory experiment AquaVIT (Section 2.4), also extreme combinations of pressure and mixing ratios, which do not occur in the atmosphere, have been set which require pressure corrections in the data analysis.

Calibrations are normally performed after each flight day or in regular intervals of a few days in order to detect potential drifts of the instrument sensitivity. Major changes of the calibrations factors occur only when modifications e.g. replacement of a detector or the mirror have been done. Typically, the calibration factors remain constant or show only a very weak trend, thus the frequent calibrations during individual missions can be used to test the reproducibility of the calibration and to increase their statistical significance. For a typical campaign, the standard deviation of c_k from the mean is ± 1:5%, and that of f_u is ± 5% (Meyer et al., 2011).

The uncertainty in f_u mainly impacts the low mixing ratio range when N_g in equation (3) becomes the same order of magnitude as N_u. For higher mixing ratios, the error of μ is determined primarily by the uncertainty of c_k. To determine the overall accuracy, we add the different contributions from the previous paragraphs. For typical operational conditions, the combined error is 5-6%. For the lowest mixing ratios we ever measured in the atmosphere (1.2 ppmv, see Chapter 4), the uncertainty f_u may double this value of the total accuracy. In particular for low mixing ratio, we further have to consider the noise or detection limit which is on the order of 0.10 - 0.15 ppmv for good instrument performance. In summary, for mixing ratios of 1-5 ppmv, an absolute uncertainly of 0.3 ppmv is a good first-order approximation for our measurements in the lower stratosphere or 7-30 % in relative terms over this range. From 5-100 ppmv, an accuracy of 6% is usually achieved. For larger mixing ratios, we have to apply a pressure correction (see above).

2.3 Field comparison of FISH with other hygrometers

Up to now, FISH was used during 13 balloon and more than 270 aircraft flights. Several of these deployments are used to compare FISH water measurements with those from other in-situ hygrometers and remote sensing sensors. A first systematic investigation is done in the SPARC Water Vapour Assessment (Kley et al., 2000): Here, the HALOE satellite data set was used as a transfer standard to many individual measurements, among others to the NOAA-CMDL frost point hygrometer, the Harvard University Lyman-α hygrometer (HWV, Weinstock et al., 2009 and references therein), the JPL Laser Hygrometer (JLH, May et al., 1998) and FISH. We refer to these instruments as their data will be discussed in this work as well. As a tendency, HALOE data appeared lower than FISH and NOAA-CMDL data in the lower stratosphere by about 5-8 %, while the HWV and JLH data showed approximately 15% higher values than NOAA-CMDL and FISH.

Since then, this tendency was confirmed in many other studies: The HALOE satellite data set (Version 19) shows a low bias also compared to actual satellite instruments, e.g. SAGE-III and MLS/AURA (e.g. Thomason et al., 2009), which again agree well with a series of CFH measurements, a spin-off frost point sonde of the NOAA-CMDL hygrometer (Vömel et al., 2007). The discrepancy between CFH and these modern satellite data on the one side and the HWV and JLH data on the other side remains also in the more recent measurements (e.g. Weinstock et al., 2009): For the very low mixing ratios in the tropics this discrepancy becomes even larger and can be as high as 50% high bias of HWV and JLH data. This explains the concerns about data accuracy as mentioned in Section 1.3 and was the demand for the laboratory intercomparison described in Section 2.4. Though no direct atmospheric

comparison between FISH and CFH measurements have been made so far, the average profiles obtained in the tropics in NH winter 2005/2006 from Northern Australia and Malaysia, respectively, agree well even for the lowest mixing ratios (see Figure 8) and do not provide any hint for a similar discrepancy as for the HWV/JLH data set.

In the last decade, FISH has made correlative measurements for the validation of several space-borne experiments, as ILAS/ADEOS (Kanzawa et al., 2002), CRISTA (Offermann et al., 2002), POAM (Lumpe et al., 2006) and MIPAS/ENVISAT (Milz et al., 2009). Also new airborne sensors were compared with FISH, as a microwave sensor (Müller et al., 2008) and a lidar (Kiemle et al., 2008). As these studies are based also on multi-instrument comparisons, often also involving the aforementioned reference instruments as transfers, the general relation of FISH data compared to those of HALOE, CFH, HWV and JLH data could be confirmed.

An important task is to assess the correlative measurements between FISH and FLASH which were used on the same aircraft during the missions discussed in this work. This intercomparison has to be restricted to clear air conditions as FISH measures total water and FLASH gas-phase water (Section 2.1). Figure 3 shows the frequency distribution of the relative difference of FISH and FLASH data from seven Geophysica campaigns as a function of relative humidity (Meyer, 2008). The majority of data is found within the combined error bars of both instruments. The low discrepancies of the mean might not be surprising, because FLASH is also calibrated with our FISH calibration bench, though less frequently. However, for individual flights much larger discrepancies are observed which exceed the combined error bars. In particular the FLASH data of the TroCCiNOx mission seem to be much more scattered.

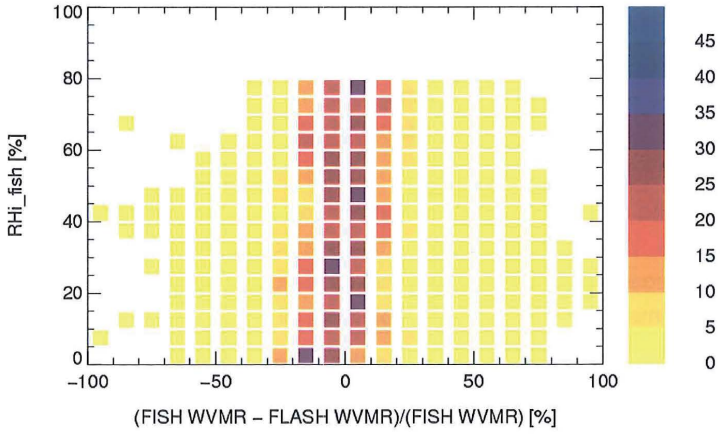

Figure 3: *Frequency distribution of the relative discrepancies between FISH and FLASH data during seven Geophysica missions (cloud-free data only).*

Due to the discrepancies for individual flights, we did a comprehensive quality check of the FISH/FLASH data set of these missions (Krämer et al., 2009) in order to allow for their consistent interpretation, in particular in the cloud studies of Chapter 5. We identified three categories of flights: 1. Data with low discrepancies remained unchanged. 2. For flights with somewhat larger discrepancies, we adjusted FLASH data to those of FISH in cloud-free sec-

tions of the flight. As FISH has a more comprehensive quality check of its data including regular calibrations after each flight, we had higher confidence in our data than in the FLASH data. 3. Flights, where discrepancies between both instruments were too large or when we could not exclude an artefact of the FISH measurement due to a recognized technical problem. Such flights were removed from the data set. So, we generated a consistent data set between FISH and FLASH, where part of the FLASH data had to be modified, and uncertain data have been removed.

2.4 The AquaVIT laboratory comparison experiment

The primary objective of AquaVIT (Water Validation Intercomparison and Tests) was establishing the accuracy of hygrometers under controlled laboratory conditions. The experiments occurred in two phases in October 2007 at the AIDA chamber of the Karlsruhe Institute for Technology (KIT). The first phase was devoted to static intercomparisons with a separate experiment each day at almost constant pressure and temperature conditions. The second phase was a week of dynamic intercomparisons, with several experiments each day under varying pressure, temperature and humidity conditions and with the absence and presence of ice clouds. An experiment description and results of the static intercomparisons are summarised in a white paper by the referees of AquaVIT (Fahey et al., 2009).

AquaVIT was a controlled, refereed, blind intercomparison of 25 different airborne field instruments. The core instrument group is comprised of eight water vapour instruments: APicT, CFH, FISH-1, FISH-2 (our Geophysica instrument), FLASH-B1, FLASH-B2, HWV, and JLH. The diode laser spectrometer APicT is an AIDA facility instrument involved in many AIDA chamber experiments (Ebert et al., 2005). The other instruments have a long history of field measurements and comparisons on balloon and aircraft platforms operating in the upper troposphere and stratosphere. Though no absolute reference instrument could be identified for AquaVIT, the APicT instrument seems to be closest to fulfil the requirements for such a reference, also based on the dynamic experiments (Fahey et al., 2009; Möhler et al., manuscript in preparation).

A summary of the core instrument intercomparison results for the static experiment series is shown Figure 4. The symbols represent the average difference within a segment from the mean water vapour value of all instruments for that segment. Note the large range of pressures for all segment groups. Summary points for all core segment results are:

10 - 150 ppmv: Good agreement occurs in this range. Except for a few segments, all the instrument segment values agree with the reference within ±10%. The instrument segment averages agree with each other within ±6%. FISH data are not yet corrected for the pressure dependence in this plot (see Section 2.2). The FLASH instruments, which unfortunately could be evaluated only in this range during AquaVIT, show the greatest segment-to-segment variability and largest differences. The other instruments show a small segment-to-segment variability (~5%) indicating good instrument stability relative to the water vapour signal level and systematic uncertainties that are constant throughout these experiments.

1 - 10 ppmv: Fair agreement occurs in this range which is the crucial one for studies of this work. All the instrument segment values agree with the reference within about ±20%. The

instrument averages over all segments also agree with each other within about ±20%. The segment-to-segment variability for each instrument is about 10% or greater indicating instrument stability issues and systematic uncertainties that are important relative to the water vapour signal value.

0.2 - 1 ppmv: Poor agreement occurs in this range. Only a few instruments reported data for these segments The instrument segment values agree with the reference and with each other within a range of about -100% to +150%. However, the differences in absolute terms are less than 0.4 ppmv. Although mixing ratios in this range occur rarely in the UT/LS, these measurements help define the detection limits and performance limits of the instruments.

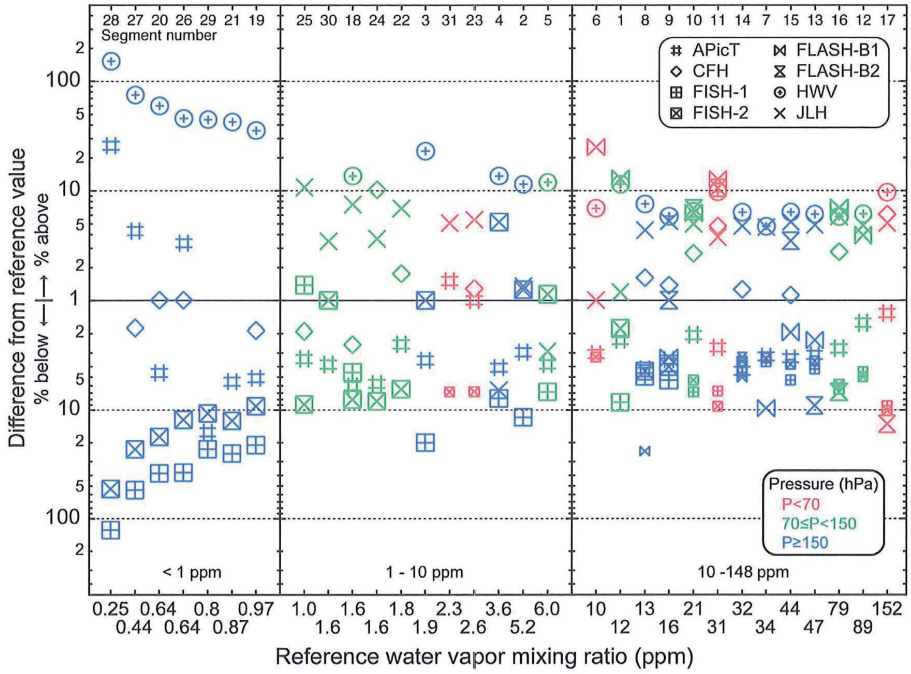

Figure 4: *Summary plot of static experiment results for the core and non-core instruments. The circle/plus symbol denotes the instrument average for all segments. Colors represent the AIDA chamber average pressure during the segment. (from Fahey et al., 2009)*

Generally, FISH data were at the lower limit of the spectrum of all instruments while those of HWV are highest. JLH is now using a new retrieval scheme that will also lower their atmospheric data published previously (R. L. Herman, personal communications, 2009). FISH data are however close to those of APicT which is regarded closest to an absolute reference. The AquaVIT results alone do not resolve the water vapour discrepancies observed in the atmosphere, as the AquaVIT discrepancies are lower; however they show similar tendencies as those reported in Section 2.3. Caution must be taken in using the AquaVIT results to infer instrument performance on moving platforms (*e.g.,* balloons and aircraft) because AquaVIT did not fully reproduce operating and sampling conditions in the UT/LS for the diverse set of instruments involved.

3 Tropical aircraft missions

In this work, data from four tropical experiments (Table 1) is presented: The Airborne Platform Experiment – Third European Stratospheric Expedition on Ozone (APE-THESEO) in February and March 1999 from Mahé, Seychelles, the Tropical Convection, Cirrus and Nitrogen Oxide experiment (TroCCiNOx) in January and February 2005 from Araçatuba, Brazil, the Stratospheric-Climate Links with Emphasis on the Upper Troposphere and Lower Stratosphere (SCOUT-O3) tropical mission in November and December 2005 from Darwin, Australia, and the African Monsoon Multidisciplinary Analysis (AMMA/SCOUT-O3) experiment in August 2006 from Ouagadougou, Burkina Faso. All four campaigns covered the convective season at the locations over the Indian Ocean, in Southern America, West Africa and Northern Australia, with the three southern hemisphere missions taking place during boreal winter and the northern hemisphere mission in Africa during boreal summer. The measurements over Africa and the Indian Ocean were the first high resolution measurements of water obtained in these particular regions.

Table 1: *Overview of tropical aircraft experiments for this study*

Experiment	Base	Time	No. of local + transfer flights	reference
SCOUT-O3	Darwin, Australia (12°S, 139°W)	31.10.-17.12.2005	8 + 12	Vaughan et al., 2008 Brunner et al., 2009 www.ozone-sec.ch.cam.ac.uk/ scout_o3/
TroCCiNOx	Araçatuba, Brazil (21°S, 58°E)	18.01.-18.02.2005	8 + 6	www.pa.op.dlr.de/troccinox
AMMA-SCOUT-O3	Ouagadougou, Burkina Faso (12°N, 1°W)	29.07.-17.08.2006	5 + 4	Cairo et al., 2010 www.isac.cnr.it/~utls/m55amma
APE-THESEO	Mahé Seychelles (4°S, 55°E)	12.02.-17.03.1999	7 + 6	Stefanutti et al., 2004

The measurements during all four missions are made from the Russian high-altitude aircraft M55 Geophysica (Stefanutti et al., 1999) with a maximum ceiling of 20 km, thus allowing to probe the full range of the tropical tropopause region by in-situ techniques. Beside the hygrometers FISH and FLASH, the aircraft was equipped with a comprehensive payload to measure a set of tracers, chemical reactive species, particles and thermodynamic parameters as summarised in the overview publications of the individual missions listed below.

The SCOUT-O3 flight routes from Darwin are displayed in Figure 5a. They include local flights in the vicinity of convection as well as long-range flights to probe the inflow and outflow region of convection and the large scale background TTL. Also the measurements during the transfer flights from and to Europe via Cyprus, Arabian Emirates, India, Thailand, and Borneo covered a wide area in the tropics. An overview on the flight patterns, objectives and meteorology of the campaign is given in Vaughan et al. (2008) and Brunner et al. (2009),

respectively. Compared to the mesoscale convective system observed over Brazil and West Africa, regularly occurring isolated storms localised over the Tiwi Islands north of Darwin, so-called 'Hector' storms (May et al., 2009 and references therein), were investigated during several flights.

Similarly, the TroCCiNOx flights include local flights to investigate convective systems (04, 05 and 18 February 2005) and long-range flights to investigate the background TTL and stratosphere (Figure 5b). Measurements were also made during the transfer route from and to Europe via Spain, Cap Verde Islands, and Recife (Brazil). The operational region in Brazil was located at the edge of the tropics, so also the mixing of tropical with extratropical air was detected during some flights (Konopka et al., 2007). Continental convective systems penetrating the tropopause have been probed by the aircraft on 04 February 2005 (see also Chaboureau et al., 2007) and 05 February 2005.

During the flights over Africa in the frame of AMMA/SCOUT-O3 (overview of flight patterns and meteorology by Cairo et al., 2010), no direct observations of deep convective systems could be made within the range of the aircraft; flight routes are given in Figure 5c. The multi-cell convective systems of the African monsoon occurred typically upwind, i.e. east of the flight routes as could be identified from satellite images. Law et al. (2010) showed that the probed air was impacted not only by uplift over Africa, but also over the Asian monsoon regions. The instrumented transfers from and to Europe covered mainly the transition to extratropical regions.

Also during the measurements in the maritime environment over the Indian Ocean during APE-THESEO (overview by Stefanutti et al., 2004) we didn't probe convective systems penetrating the tropopause. However, one flight was dedicated to investigate the region above a tropical cyclone (Cairo et al., 2008), and frequent cirrus layers at the tropopause, sometimes of convective origin, have been detected (Chapter 5). During this mission, for the first time we successfully operated the strategy of so-called tandem flights, i.e. we used lidar measurements onboard the DLR Falcon aircraft to direct the Geophysica into regions with thin cloud layers. Figure 5d shows the flight routes over the Indian Ocean, the transfers from Italy via Amman and Djibouti were instrumented flights as for the other missions.

As a complement to the tropical cirrus data, the studies in Chapter 5 make also use of data from our extratropical airborne experiments during which warmer and thicker cirrus were probed. They include our measurements for ENVISAT validation, the Cirrus campaign series at mid-latitudes and the polar experiments POLSTAR and EUPLEX. Beside from the Geophysica, data were obtained from the DLR Falcon and the Lear Jet managed by Enviscope GmbH, Frankfurt. Details of these missions are given in Schiller et al. (2008a) and Krämer et al. (2009) and references therein.

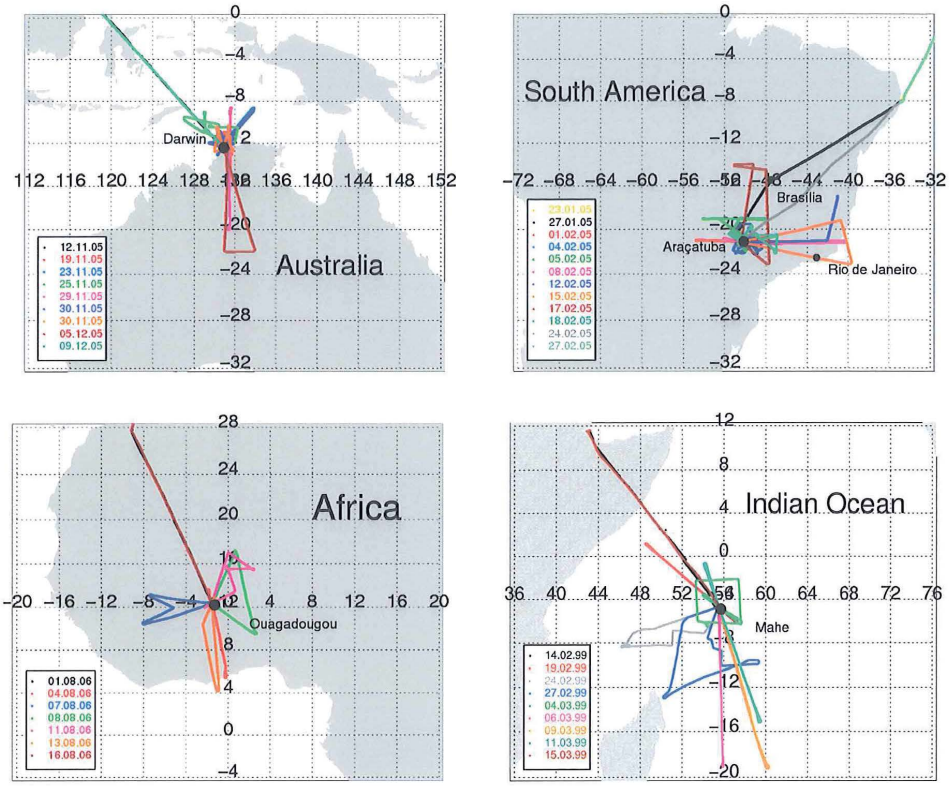

Figure 5: *Routes of local flights during (a) SCOUT-O3 with operation base in Darwin, Australia (b) TroCCiNOx with operation base in Araçatuba, Brazil (c) AMMA/SCOUT-O3 with operation base in Ouagadougou, Burkina Faso and (d) APE-THESEO with operation base from Mahé, Seychelles. Parts of the transfer flights to and from Europe are included. (panels a-c from Schiller et al., 2009)*

4 Water in the tropical tropopause layer

Active dehydration or hydration are typically identified by the coincidence of particle occurrence and characteristic supersaturated or subsaturated air masses. The tropopause, in a simplified view defined by the cold point, i.e. the temperature minimum, is a preferred altitude where such processes occur as RH_{ice} becomes highest. The coincidence of temperature and water entry variability reviewed in Chapter 1 clearly reflects the cold trap function of the tropical tropopause. On a seasonal time scale, Mote et al. (1996) identified a water-temperature link in satellite data, and he denoted the imprint of the temperature at the tropical tropopause on the water entry a 'tape recorder signal'. Interannual variations of temperature and water at the tropical tropopause on a global scale were studied by Randel et al. (2004), Fueglistaler et al. (2005) and Fueglistaler and Haynes (2005).

In this Chapter, I use our high-resolution data from different seasons and locations to refine these concepts and to derive the underlying processes and their relative importance for the water entry into the stratosphere. For this purpose, I use only our total water measurements plus temperature information in comparison with the so-called water reconstruction modelling method. Hereby, the microphysical concepts are kept very simple – their discussion is given in Chapter 5.

4.1 Vertical profiles of H_2O

Here, the vertical distribution of water in the TTL is discussed and compared for the the different campaign locations and seasons. All flights include measurements of at least two profiles during ascent and descent; most of the local flights include additional profiling information from aircraft dives. The vertical information may, according to the flight pattern, be gathered over horizontal distances of several hundred kilometres. As vertical coordinate, usually potential temperature θ is used; in these coordinates, the tropical tropopause is often found near θ = 380 K, corresponding to an altitude of 17 km (e.g. Fueglistaler et al., 2009).

The location of the cold-point tropopause, of the hygropause which is the altitude of the minimum water mixing ratio, and of the vertical extent of saturated air is displayed for the individual profiles of the APE-THESEO campaign in Figure 6. For the local flights over the Indian Ocean, the altitude of all three quantities coincides at an altitude range around 380 K (Beuermann, 2001; MacKenzie et al., 2006), as expected for this season (see below). The frequent occurrence of saturation, often accompanied by cloud occurrence (see Section 5), identifies this region as preferred one for active, ongoing dehydration. Minimum water mixing ratios were often below 2 ppmv indicating that beside the known dehydration potential over the Western Pacific also over the Indian Ocean region, freeze-drying down to the lowest mixing ratios may occur. Fueglistaler and Haynes (2005) pointed out that this particular year 1999 showed extremely low tropopause temperatures in that region (compared to higher ones in the following one) which agree with the observed low mixing ratios observed at the tropopause.

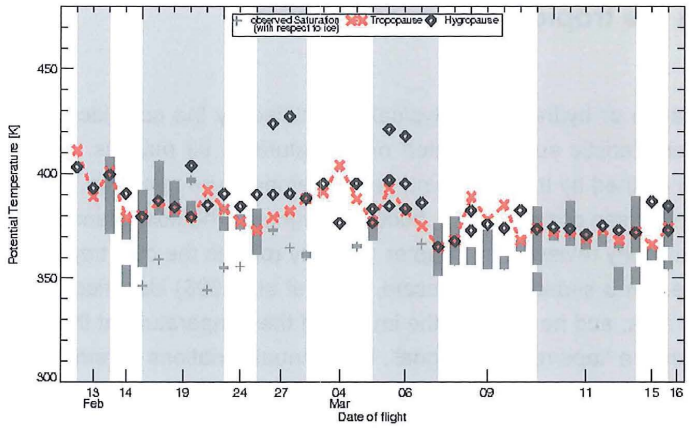

Figure 6: *Potential temperature of the cold-point tropopause (crosses) and the hygropause (diamonds) for each ascent and descent of the Geophysica during the APE-THESEO campaign. Additional minima in total water are shown as diamonds. Also shown (grey bars) is the section of each profile that is saturated with respect to water ice. (update from MacKenzie et al., 2006)*

Corresponding Figures of individual profiles for the other three campaigns are evaluated in Silva dos Santos (2008). In Figure 7, the measured water profiles are displayed for these three campaigns, colour-coded with respect to RH_{ice} (Schiller et al., 2009). The profiles are rather compact around a mean value – except data obtained in clouds and specific situations to be discussed in Section 4.3.

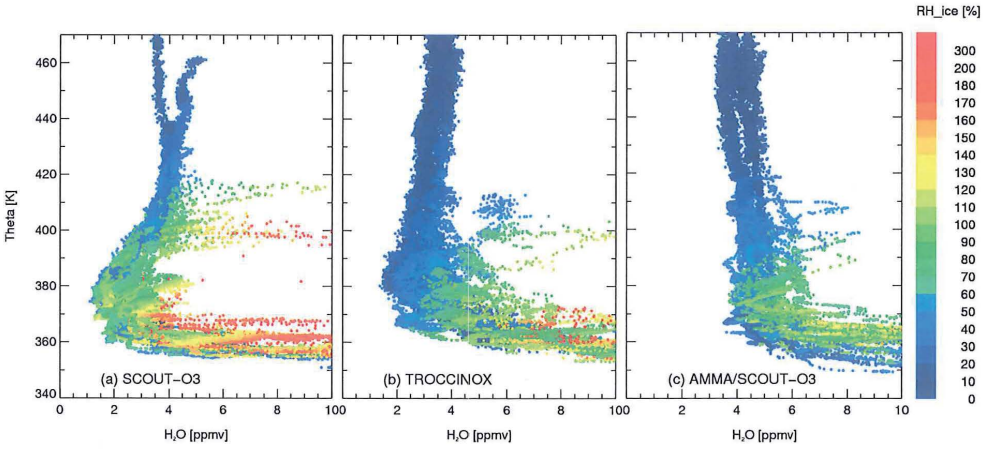

Figure 7: *Vertical profiles of total water during the tropical aircraft campaigns (a) SCOUT-O3 in Northern Australia (November 2005), (b) TroCCiNOx in Brazil (February 2005), and (c) AMMA/SCOUT-O3 in West Africa (August 2008). Colour code denotes RH_{ice}. (from Schiller et al., 2009)*

Water profiles during SCOUT-O3 are similar to those during APE-THESEO with lowest mixing ratios of less than 2 ppmv at potential temperatures θ = 370-380 K, almost coinciding with the local cold point tropopause which was observed around 375 K on average for this period

and location (Brunner et al., 2009). The corresponding temperatures were low at these altitudes, i.e. on average -85° C, therefore frequently RH_{ice} close to saturation or clouds were observed in the vicinity of the tropopause. Striking features are layers of high H_2O and cloud occurrence above the tropopause from observation of deep convection above Tiwi Island, the Hector storms (see Section 4.3). High RH_{ice} at the cold point tropopause is indicative for effective freeze-drying down to very low mixing ratios in this region and season.

Also during TroCCiNOx, very low mixing ratios were observed, in few cases also close to 2 ppmv. The average minimum is found at slightly higher altitudes, but still close to the average cold point tropopause, which was found between 370 and 380 K, depending on the actual conditions. As the most obvious difference to the SCOUT-O3 observations, mean cold point temperatures were higher, i.e. -79° C; thus most of the measurements were made at subsaturated conditions without clouds. Only for the flights on 04 and 05 February 2005 when convection reached the tropopause, clouds and high RH_{ice} were observed in that region. Again, enhanced water vapour and ice particles were injected into the stratosphere up to about 415 K during these events.

The AMMA/SCOUT-O3 profiles look very different to those of the three other campaigns, both in absolute values and in the stratospheric gradient. At the cold-point tropopause with an average location at 370 K, the water mixing ratio has a mean value of 5 ppmv and shows a pronounced change of the slope, but decreases further in the stratosphere. Balloon measurements in the same region (Khaykin et al., 2009) show the H_2O minimum at approximately 20 km altitude, corresponding to the maximum ceiling of the Geophysica aircraft from which our data are obtained. Here, the mean mixing ratio obtained from the balloon instrument is 4.4 ppmv and thus consistent with our measurements at these altitudes (4.1 ppmv). Temperatures at the tropopause are significantly higher than during SCOUT-O3 and APE-THESEO but similar to those from TroCCiNOx. With the higher H_2O values, RH_{ice} frequently is close to 100% in a thin layer around the cold point, sometimes accompanied by cirrus cloud occurrence. Though no Geophysica flights directly above deep convection were made during AMMA/SCOUT-O3, layers of enhanced H_2O above the tropopause are detected in three profiles.

Figure 8 summarises the average water profiles obtained during the four tropical Geophysica missions. Hereby, data in convection-induced ice clouds have not been included as these phenomena lead to a local moistening. Figure 8 also shows CFH measurements over Indonesia during the SOWER campaign in early January 2006 (Vömel et al., 2007), which are obtained close to our SCOUT-O3 data in a nearby region. The averaged SCOUT-O3 and SOWER profiles agree well above 380 K in terms of absolute values and slope, at lower altitudes the local conditions are likely the reason for slightly higher mixing ratios over Darwin with a strong convective impact. Thus they corroborate the consistency of FISH and CFH measurements also in atmospheric measurements. Also the profiles of Kelly et al. (1993) obtained during the STEP campaign January 1987 from Darwin are very close to the SCOUT-O3 profiles in quantity and slope. The TroCCiNOx and APE-THESEO data show slightly lower values above 410 K compared to SCOUT-O3. As these campaigns were carried out three months later in season, the difference would be consistent with an upward propagation of the dehydration signal, the so-called tape recorder (Mote et al., 1996): Using

a clear-sky cooling rate of 0.6 K/d for this region (e.g. Corti et al., 2005), air parcels are lifted from the cold point tropopause to the 410-430 K region in this time.

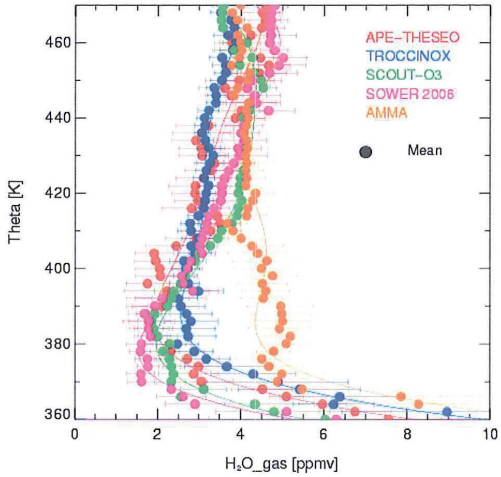

Figure 8: *Comparison of mean water vapour profiles of the APE-THESEO, TroCCiNOx, SCOUT-O3, AMMA/SCOUT-O3 and SOWER mission (from Schiller et al., 2009).*

We cannot exclude, however, that a year-to-year variability is overlaid to this phenomenon (Section 4.2), and the regional influence at these altitudes leads to zonal asymmetries, but to first order the data reflect the upward propagation of the tape recorder signal with season. Close to the tropopause, the H_2O mixing ratios during TroCCiNOx are higher than the very low values during SOWER, SCOUT-O3 and APE-THESEO and therefore account for moister and warmer conditions at the edge of the tropics over South America. The AMMA/SCOUT-O3 obtained in northern hemispheric summer are higher by about 2-3 ppmv at 380 K compared to the other campaigns, consistent with the higher water vapour entry in that season and similar to e.g. the historical Panama data in September 1980 by Kley et al. (1982) and sonde data from Costa Rica (Vömel et al., 2007). Above 410 K, the absolute mixing ratios are very similar for all campaigns (including the SOWER, Panama and Costa Rica data), thus the tape recorder amplitude is already smeared-out or masked by regional or year-to year variability. However, the different slopes between the northern hemispheric summer and winter data are still indicative for the upwelling of the freeze-drying signal from the cold point region with season.

4.2 Dehydration at the tropical tropopause

For the local flights during APE-THESEO and SCOUT-O3, saturation conditions were observed frequently in a broad altitude band around the cold point, indicative for local dehydration down to the very low mixing ratios of 2 ppmv or less. For AMMA/SCOUT-O3, saturation is reached up to the cold point in part of the profiles, and for TroCCiNOx, H_2O mixing ratios at the tropopause were usually lower than the local saturation. Therefore, in many cases the corresponding freeze drying events must have occurred earlier and at different locations.

We therefore use backward trajectories ending at the flight paths of the three missions to determine the temperature history of the observed air parcels and to reconstruct its water content (Schiller et al., 2009). The trajectories are calculated using the Chemical Lagrangian Model of the Stratosphere (CLaMS; McKenna et al., 2002), which is driven by ECMWF meteorological fields. For the vertical parameterisation of the tropopause region, a hybrid coordinate is chosen as described by Konopka (2007). Calculations are made for different trajectory lengths of 10 and 30 day, respectively. A longer trajectory length typically results in lower saturation mixing ratios for two reasons: first, the likelihood to encounter very low temperature regions increases, and second, due to diabatic ascent of air, a larger part of the trajectories has passed the cold point region before.

We tested the sensitivity of saturation mixing ratio along the trajectories at which the freeze drying occurs, considering a relative humidity over ice RH_{ice} = 100% and 130%, respectively (for more details of this topic see Chapter 5). Hereby, the mixing ratio at the end of the trajectory can be changed by up to 0.3 ppmv, providing that a major dehydration had occurred (see below).

In a first step, I compare the minimum saturation mixing ratio along the trajectories with the measured H_2O. Herby, the average profiles of the local flights and tropical parts of the transfer flights are used. In a second step, the trajectories are initialised with climatological data from the HALOE satellite experiment (Grooß and Russel, 2005) to allow for a complete so-called reconstruction of water.

4.2.1 Saturation history

The first comparison of the minimum saturation mixing ratio with the data gives the following main results, for a more detailed discussion see Schiller et al. (2009, reprinted in the Appendix). The data can be divided in three altitude bins, which vary between the different campaigns. Below the tropopause, the calculated minimum saturation data along the backward trajectories are lower than the measured H_2O profiles. The reason is that the measurements are frequently affected by local convection moistening the lower TTL (see also Section 4.3 and 4.4), a process which is not considered by the trajectory analysis.

The second bin is the altitude range around the tropopause where the calculated saturation mixing ratios agree with the measured ones. For SCOUT-O3, this bin ranges from 370 to 400 K, with very little change when the trajectory length is increased from 10 to 30 days. This implies that dehydration is ongoing in the region of the measurements or nearby (as for APE-THESEO and SCOUT-O3), and is extended even to the first kilometres above the tropopause. Thus also moister air injected by convection above the tropopause (see Section 4.3) may be freeze-dried back to very low mixing ratios. The frequent saturation shown in Figure 7a corroborates these findings. For TroCCiNOx, a large change of the saturation mixing ratio along the backward trajectories is evident when increasing their length from 10 to 30 days. This implies that the set point of the low water vapour at these altitudes dates back up to a month and likely from a remote region (see below). The reported frequent subsaturation close to the cold point and above (Figure 7b) already showed that the operational area at the edge to the subtropics is not an area of active dehydration – at least when air with low mixing

ratios is advected. For the AMMA/SCOUT-O3 observations, saturation along the backward trajectories can explain the H_2O measurements only up to the cold point around 370 K. Even the minimum saturation over 30 days does not approach the measurements much closer in the stratosphere anymore.

In the third bin, higher in the stratosphere, the minimum saturation mixing ratios do no longer match the observations, indicating that the freeze-drying must have occurred longer than a month ago as already discussed in the context of the tape recorder in Section 4.1.

4.2.2 Tropical regions of dehydration

The backward trajectory calculations are suited to identify the tropical region where saturation at the lowest mixing ratio preferably occurs. Figure 9 shows the cold points along the 30-day backward trajectories for the three campaigns in the potential temperature range 375-410 K, colour-coded for the corresponding minimum saturation mixing ratio if it agrees with the observation within an interval of ± 0.5 ppmv.

The lowest temperatures for the SCOUT-O3 measurement (Figure 9a) occur close to the aircraft tracks in the equatorial Western Pacific. This region has been identified also in previous studies as the tropical region with the highest dehydration potential in this season (e.g. Fueglistaler et al., 2005).

As discussed above, for TroCCiNOx only saturation along longer trajectories can explain the observed low mixing ratios over Southern Brazil. The air masses probed by the aircraft have been dried in regions more equatorwards (Figure 9b), in particular over South America and over the Western and Central Pacific. Also Fueglistaler et al. (2005) identified these two regions to be coldest. Our measurements at the edge to the subtropics show that the dehydration to lowest mixing ratios at these cold spots is advected also to remote regions with higher temperatures.

For AMMA/SCOUT-O3, the air masses probed over Africa generally origin from the East (Figure 9c). Lowest temperatures corresponding to a saturation mixing ratio of 4-6 ppmv occur over India and the Gulf of Bengal. Thus, the H_2O mixing ratios close to the cold point observed over Africa are broadly consistent with the colder set point in the southern flank of the Asian monsoon. So the Asian monsoon is not only a major source of water vapour as concluded from previous studies (e.g. Randel and Park, 2006; James et al., 2008), its cold point characteristics at the same location also adjust the entry of water vapour into the stratosphere and determine the water vapour concentrations in the downwind regions over Africa.

Figure 9 (next page): *Location of coldest temperatures along backward trajectories (θ = 375-410 K) with end points along the flight tracks during (a) SCOUT-O3, (b) TroCCiNOx and (c) AMMA/SCOUT-O3 (considered flight routes including part of the transfers displayed by grey triangles). The minimum saturation mixing ratio along the backtrajectories if corresponding to the aircraft measurement is marked in colour. (from Schiller et al., 2009)*

SCOUT–O3

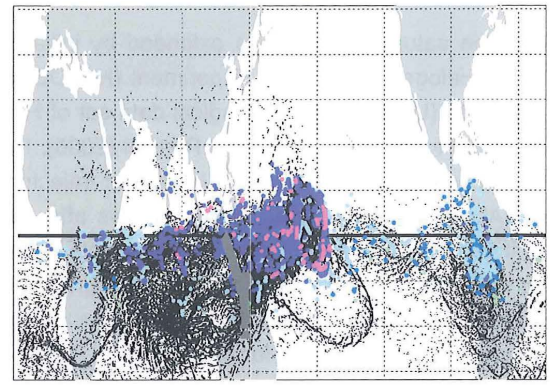

1.0 1.7 2.4 3.1 3.8 4.5 5.2 5.9 6.6 7.3 8.0

H_2O [ppmv]

TroCCiNOx

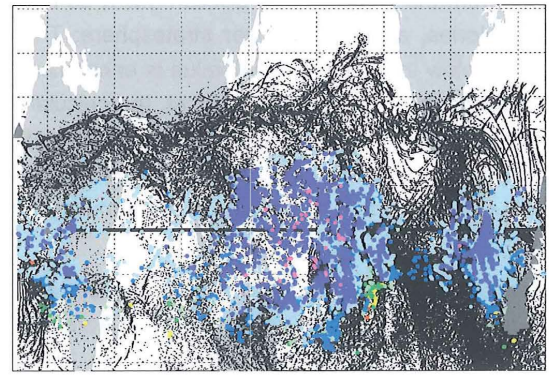

1.0 1.7 2.4 3.1 3.8 4.5 5.2 5.9 6.6 7.3 8.0

H_2O [ppmv]

AMMA

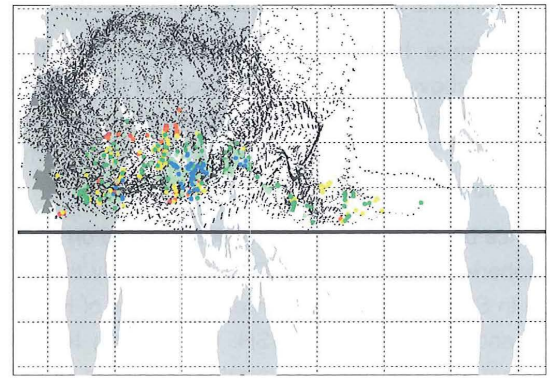

1.0 1.7 2.4 3.1 3.8 4.5 5.2 5.9 6.6 7.3 8.0

H_2O [ppmv]

4.2.3 Reconstruction of water with HALOE climatological data

Now, the discussion of the saturation history is extended by initialising the trajectory end points with data from the Halogen Occultation Experiment (HALOE) onboard the Upper Atmosphere Research Satellite (UARS). A climatological data set of H_2O of this experiment is compiled for the years 1991 to 2002 in Grooß and Russell (2005). For the initialisation, the zonal average for the respective latitude bin at the backward trajectory end point is chosen. Figure 10 shows the HALOE-initialised water vapour profiles after modifications by 10-day and 30-day backward trajectory calculations (green and red dots, respectively), compared to the actually measured FISH data for the three tropical campaigns. The simulations are done for RH_{ice} of 100% (crosses) and 130% (circles). The black line in the main panels denotes the mean HALOE climatological H_2O profile used for initialisation.

For SCOUT-O3 (Figure 10a), the change between the HALOE initialisation profile (black line) and the reconstructed mixing ratios at the observation point (green and red dots, for trajectory lengths of 10-day and 30-day, respectively) is largest. The large modifications below 410 K are already expected from the discussion in Section 4.2.1, as the cold point is frequently reached along the trajectories, also in the lower stratosphere: The fraction of trajectories along which a cold point below the HALOE initial value is encountered, is 100-10% in the θ-range 380-410K (right subpanel). Above the cold point, the calculated H_2O profiles (30-day trajectories) match extremely well the mean profiles measured by FISH, and those for the shorter 10-day history are only slightly higher. Below the cold point, recent convection has enhanced the actual H_2O mixing ratio compared to the simulated values, as already discussed above.

The TroCCiNOx comparison provides also a good agreement between the reconstructed and measured H_2O mean profiles above θ = 380 K (Figure 10b). Here, the modifications between the climatological HALOE profiles along the trajectories are by far weaker than for the SCOUT-O3 period, i.e. only 50-10% of the trajectories at 380-400K meet a cold point below the HALOE initial value (right subpanel). Below 380 K, the measured mean H_2O mixing ratio is higher than the reconstructed value, indicative for additional recent moistening due to vertical mixing along the subtropical jet (Konopka et al., 2007; Section 4.4).

For AMMA/SCOUT-O3 (Figure 10c), virtually no change of the initial HALOE profile occurs along the back trajectories above 375 K. Here, the slope of the profiles is very similar, though the HALOE climatological data are lower by approximately 0.4 ppmv (or 10%) above 390 K. Good agreement is found at 370-390K close to the tropopause, while below the measurements are again higher than the simulations.

The systematic difference between the reconstructions, based on HALOE data, and the FISH profiles in the stratosphere during AMMA/SCOUT-O3 is likely caused by instrument uncertainties. As discussed in Section 2.3, HALOE measurements of H_2O tend to have a low bias to other hygrometers and in particular to FISH. Considering this low bias of the HALOE measurements on the order of 8%, the agreement between the simulations and FISH measurements improves for the AMMA/SCOUT-O3 case. Initialisation with higher HALOE data would however not change the H_2O reconstruction for the TroCCiNOX and SCOUT-O3 to a larger extent, as most of these data are lowered to the saturation mixing ratio at the minimum

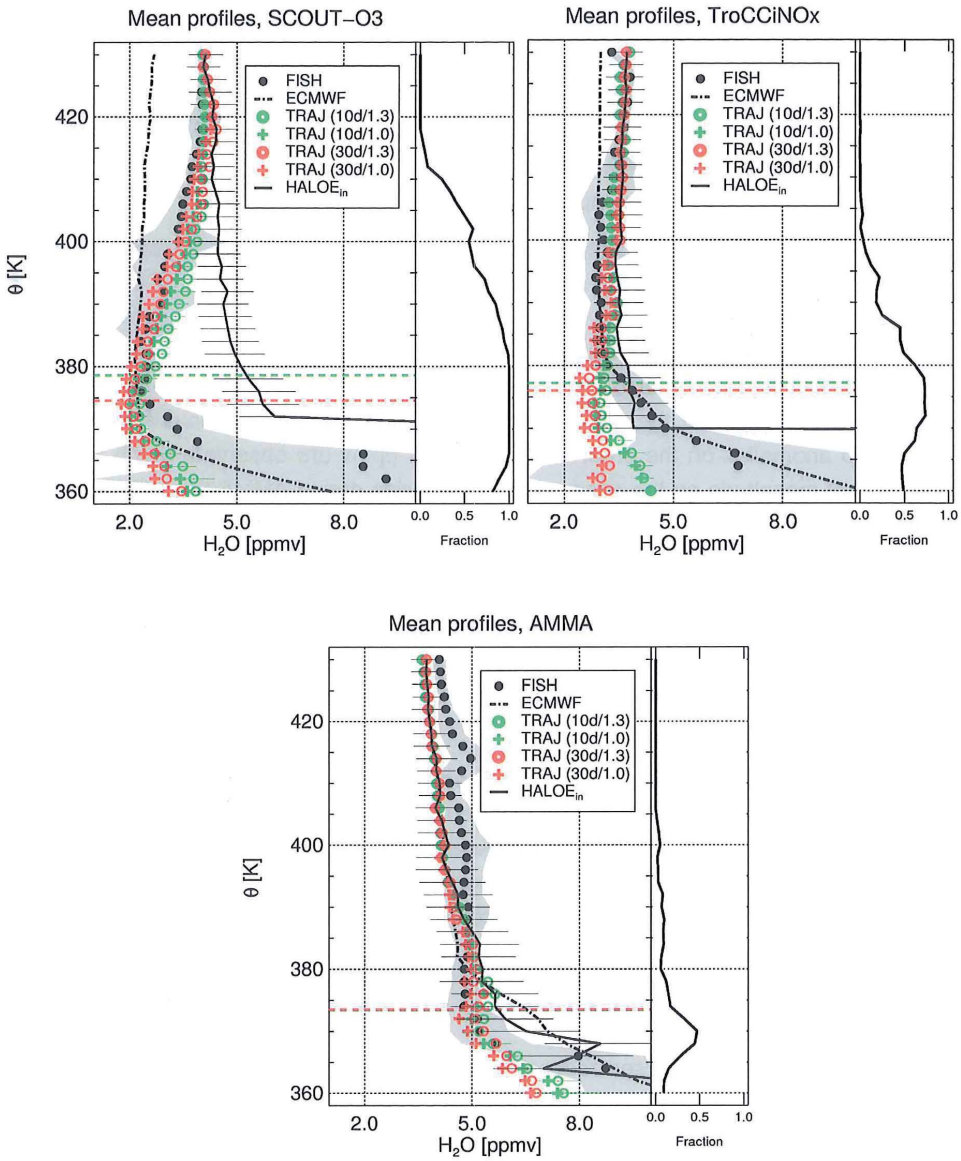

Figure 10: *Comparison between mean measured H_2O profiles and simulated ones; freeze-drying along the trajectories to RH_{ice} = 100% (crosses) and 130% (circles). Backtrajectory calculations are initialised with H_2O climatological data from the HALOE satellite experiment (green dots based on 10-day trajectories, red dots on 30-day trajectories). The black profiles show the mean HALOE profiles and their standard deviation used for initialisation. The dashed-dotted profile is the averaged ECMWF specific humidity value interpolated to the flight tracks. The right subpanels show the fraction of trajectories along which a cold point below the HALOE initial value is encountered.*

cold point along the back trajectories anyway. Therefore, our tropical measurements likely confirm the previously found moderate low bias of HALOE data compared to FISH measurements, which however is on the order of the combined errors. The mean FISH profiles agree also well with those of the AMMA balloon data using the FLASH-B hygrometer (Khaykin et al., 2009), the slight discrepancy at 19-20 km of 0.2 ppmv is even lower than the total accuracy of both instruments implies (approx. 8% for FISH and 10% for FLASH-B).

A deviation of our FISH measurements from simulations using a climatological initialisation may also be caused by atmospheric variability – in particular for the AMMA/SCOUT-O3 case when the H_2O concentration is not altered along the back trajectories for a large altitude range. Randel et al. (2004) discussed, based on HALOE data, interannual changes of stratospheric water vapour which could be attributed to changes of temperatures at the tropical tropopause associated with the quasi-biennial oscillation and El Niño-Southern oscillation. Hereby, H_2O anomalies on the order of a few tenths ppmv are observed, which are of the same order of magnitude as the observed discrepancies during AMMA/SCOUT-O3. Recent satellite observations (Jones et al., 2009) indicate that water vapour in the tropical lower stratosphere has approached values for our observation period in 2005/2006 which are comparable to the mean values of the period considered in the HALOE climatology of Grooß and Russel (2005). In summary, the observed discrepancies between HALOE and FISH data during AMMA/SCOUT-O3 in the stratosphere may be caused by the interannual variability of water vapour entry, though there is no quantitative assessment of such a possible effect possible for the moment.

Beside the interannual variability, also a zonal asymmetry may have caused the observed discrepancies during AMMA/SCOUT-O3, as discussed in Schiller et al. (2009) extending the original HALOE climatology by Grooß and Russel (2005) to zonally resolved data. From the HALOE perspective, the influence of the monsoon regions become apparent but are limited to a few tenths of ppmv in the TTL above the cold point, i.e. 3-9% additional water compared to the zonal mean. Hereby, the direct contribution of the African monsoon might still be overestimated as this region is located downwind of and therefore impacted by the Asian monsoon region.

In summary, the HALOE-initialised reconstruction of water shows good agreement with the SCOUT-O3 and TroCCiNOx data. The frequent dehydration events in the trajectory history explain, why the regionally observed data differ significantly from the initial, climatological satellite profiles. For AMMA/SCOUT-O3, the initial HALOE profile remains almost unchanged in the stratosphere by reconstruction. The known bias between HALOE and FISH is sufficient to explain the observed discrepancies of about 10%. Comparison of climatological data with regional ones allows us to estimate an upper limit of the possible impact of phenomena which are not considered in the reconstruction, in particular that of local convection (Chapter 6).

4.3 Moistening by deep convection

In Figure 7, layers of enhanced water vapour are visible below and above the tropopause which we already attributed to the impact of deep convection. In Figure 11, the ice water content (IWC) calculated from the difference of FISH and FLASH measurements during two flights of TroCCiNOx and four flights of SCOUT-O3 is displayed. High IWC is found below the tropopause (380 K potential temperature) in the main convective outflow, but also volume mixing ratios of particulate water corresponding to up to 50 ppmv at 400 K and up to 5 ppmv at 415 K are measured. This is considerably higher than previously reported IWC of less than 2 ppmv above 400 K (Kelly et al., 1993), also from measurement out of Darwin. Our IWC data are corroborated by in-situ and lidar measurements of particle from the Geophysica (Corti et al., 2008; de Reus et al., 2009).

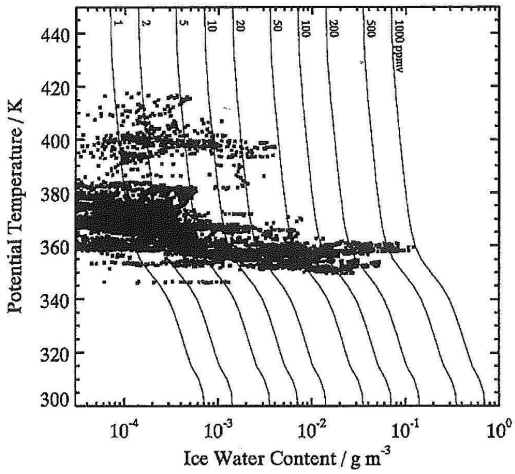

Figure 11. *Ice water content observed in deep convective systems during two TroCCiNOx and four SCOUT-O3 flights. (from Corti et al., 2008).*

The major outflow of convection below the cold point results in a moistening of the lower TTL as already concluded in Section 4.2.1. However, this additional water vapour does not result in an increased transport of H_2O into the stratosphere, as it is trapped at the cold point during the subsequent ascent. As an example, observations in the aged outflow of a strong Hector event on 30 November 2005 showed saturated air masses over a large area at and below the cold point at mixing ratios of 2-4 ppmv with only a few remnants of particle plumes. Therefore, already a few hours after a convective event, the air masses from the outflow might be freeze-dried back to the saturation conditions.

Contrary, the particles and layers of enhanced water found above the cold point potentially moisten the stratosphere. In Corti et al. (2008), we first discuss hypotheses of their origin. We can exclude that they stem from unintended sampling of the own contrail or eliminate the few cases (less than 3%) from the data in Figure 10. Another explanation for the observed ice particles could be in situ nucleation and growth. Adiabatic cooling of air masses lifted above convective systems can lead to supersaturation, inducing the formation of so-called pileus clouds. This is contradicted by our observations as in all observed cases, the ice parti-

cles have been embedded in subsaturated air. We therefore conclude that convective transport is the sole possible explanation for most of the ice particles observed in the stratospheric overworld. The most direct evidence for convective activity is given by the lidar observations showing the remnants of a convective plume. As shown in Schiller et al. (2008), the IWC of these clouds is significantly higher than the climatological range of IWC from other observations at these low temperatures (Section 5.1.2). Such high IWC are therefore indicative of rapid transport from the troposphere as in convection.

Box model calculations suggest that evaporation of these ice particles have a moistening effect on the stratospheric water vapour content (Corti et al., 2008). Same conclusions are drawn in the study by de Reus (2009). In contrast, there are no indications of convective dehydration in the stratosphere as postulated e.g. by Danielsen (1993) and Sherwood and Dessler (2001), i.e. no anomalously low water vapor mixing ratios were found. They confirm previous model calculations by Jensen et al. (2007) postulating such a moistening effect if particles are injected in subsaturated air above the tropopause.

Independently, striking evidence for persistent moistening is derived from the measurements over Africa when layers of enhanced water up to 420 K are detected in single profiles (Figure 8c). In contrast to the observations during SCOUT-O3 and TroCCiNOx, these measurements were not obtained in the vicinity of deep convection and no particles are detected in these layers. On the other hand, back trajectory calculation with CLaMS show that these observations were made downwind of large mesoscale convective systems detected with good coincidence in time and location by the Meteosat-08 observations (Silva dos Santos, 2008). These observations, which are similar to those reported from AMMA balloon-borne measurements in the same region (Khaykin et al., 2009), provide evidence that deep convection injects water irreversibly above the cold point, as these layers with H_2O enhanced by 2-3 ppmv can still be detected about 10-20 hours after the convective event in subsaturated air without remnants of particles. Therefore, it can be excluded that such injections occur only as a temporary lifting above the tropopause without mixing with the environment as well as a complete sedimentation of particles back to tropospheric altitudes.

The observed layers with enhanced water vapour above the cold point are a highly localised phenomenon on horizontal scales of several 10 km. Probing these events above Tiwi Island during SCOUT-O3, identified an area on the order of 2000 km^2 (50 km diameter) with particles above the tropopause. Similarly, during AMMA the layers occurred only in single profiles while the next profile a few 100 km apart showed again the undisturbed background profile. The observations during the three campaigns, also taking into account the balloon observations by Khaykin et al. (2009), are quite frequent. On the other hand, their fraction of the total number of measured profile has to be regarded as a biased upper limit, since the flight programme in all missions was focussed on the observation of convective systems and their outflow regions.

4.4 Model-observation-based studies of the TTL structure

In this Section, I summarise a number of modelling studies in which our data from the tropical campaigns are used to test these new models. They include two Lagrangian model tools, two Eulerian models and two mesoscale models. Each of them includes new concepts, hypotheses or parameterisations for specific processes in the tropics, both for transport and microphysics. Confidence in their validity is based on such comparison with experimental data and leads to an improved understanding of the TTL and processes occurring there.

To investigate transport across TTL in the course of our tropical missions, a new version of the Jülich Chemical Lagrangian Model of the Stratosphere (CLaMS; McKenna et al., 2002) was developed. In this new version, the stratospheric model has been extended to the earth surface (Konopka et al., 2007). Above the tropopause, the isentropic and cross-isentropic advection in CLaMS is driven by ECMWF winds and heating/cooling rates derived from a radiation calculation. Below the tropopause the model smoothly transforms from the isentropic to hybrid-pressure coordinate and, in this way, takes into account the effect of large-scale convective transport as implemented in the ECMWF vertical wind. As with other CLaMS simulations, the irreversible transport, i.e. mixing, is controlled by the local horizontal strain and vertical shear rates. These concepts have been extended by Plöger et al. (2010).

Stratospheric and tropospheric signatures in the TTL can be seen both in the observation and in the model. The composition of air above ≈350 K is mainly controlled by mixing on a time scale of weeks or even months. Based on CLaMS transport studies where mixing can be completely switched off, Konopka et al. (2007) deduce that vertical mixing, mainly driven by the vertical shear in the outflow regions of the large-scale convection and in the vicinity of the subtropical jets is necessary to understand the upward transport of the tropospheric air from the main convective outflow around 350 K up to the tropical tropopause around 380 K. This mechanism is most effective if the outflow of the mesoscale convective systems interacts with the subtropical jets.

Our measurements of H_2O during TroCCiNOx, together with those of other tracers, were ideally suited to test these new concepts of transport in the TTL. In particular data from two flights in the vicinity of the subtropical jet with convective impact agreed well with the CLaMS simulations and therefore gave confidence in the validity of the new transport schemes in CLaMS (Konopka et al., 2007).

Plöger et al. (2011) extend the reconstruction of water vapour (Section 4.2) testing different trajectory schemes, i.e. kinematic and diabatic 3-month backtrajectories based on ERA-Interim data and using ozone as an independent tracer. The water vapour reconstruction is nearly insensitive on the chosen trajectory scheme, which implies that dehydration in the coldest regions is effective for different upwelling and dispersion. However, ozone is found to be highly sensitive on the chosen transport scheme and thus a suited tracer to evaluate e.g. vertical transport in the TTL.

The improvement of CLaMS vertical transport in the tropics, which has been used for our water reconstruction in Section 4.2, is also obvious from comparison to the specific humidity product of ECMWF analyses, in the following denoted as SH_{ECMWF} (Figures 10a-c, dashed-

dotted black lines). As a general tendency, SH_{ECMWF} underestimates the measured H_2O mixing ratios in the stratosphere by 0.5 – 2 ppmv, with larger discrepancies at higher altitudes (Schiller et al., 2009). Similar differences between matched HALOE/MLS data and SH_{ECMWF} (ERA-40 analysis) are also apparent in a zonal mean climatology (Dethof, 2003; Figure 3 therein), i.e. a larger bias and less steep gradients of SH_{ECMWF} compared to the satellite zonal mean data for the tropical SH in January and a somewhat better agreement for the AMMA/SCOUT-O3 latitudes and season at higher mixing ratios. Comparing the water tape recorder of ECMWF products and that of the HALOE climatology, a too effective vertical transport rate in ECMWF assimilations seems to be the main reason for the discrepancy between SH_{ECMWF} and observations (P. Konopka, private communications).

Ren et al. (2007) developed the Lagrangian air-parcel cirrus model (LACM) to reconstruct water and compared simulations to our TroCCiNOx data. The transport is based on different Lagrangian algorithms to which a microphysical scheme is hooked-up. Further, they optionally account for rehydration by deep convective systems in the TTL. Similar to our CLaMS simulations, the reconstruction below the cold point results in a dry bias if no rehydration by convection is considered. If this feature is added in LACM, then the reconstruction becomes much closer to the FISH observations. Also the LACM simulations provide an improvement of water constructions at and above the tropopause, as for our CLaMS reconstructions. In Horseman et al. (2010), the LACM algorithm is combined with a full chemical transport model and first simulations compared to our SCOUT-O3 water data. Again, the water reconstruction yielded encouraging results at and above the tropopause, but the authors also identified necessary improvements in the treatment of the vertical winds in their model.

Palazzi et al. (2009) use runs with a Chemistry-Climate Model (ECHAM5/MESSy) to investigate chemical tracer profiles in the TTL, among others that of water. The comparison with data from our four tropical aircraft missions is done for average profiles and probability distribution functions. The model estimate of the thickness of the interface region between tropospheric and stratospheric regimes agrees well with average values inferred from observations. As the measurements below the tropopause are influenced by regional scale variability, local transport processes as well as deep convection, they are less accurately captured by the model. The tropopause minimum and values in the higher stratosphere are well reproduced for APE-THESEO, SCOUT-O3, and TroCCiNOx, however the AMMA/SCOUT-O3 simulations have a significant low bias compared to the measurements. A corresponding low bias was also detected for the same model compared to HALOE satellite data in a study by Lelieveld et al. (2007). Tost et al. (2010) also use the ECHAM5/MESSy model for their studies testing different convection schemes. Again, they used our SCOUT-O3 data, including those obtained from the Falcon aircraft operating at lower altitudes, and found a general good agreement. From the comparisons, also with other tracers, they assessed the quality of the different applied convection schemes.

Finally, our high-resolution data have been used in studies of specific convective systems using mesoscale-models. These nested models with resolution down to several 100 m are designed for the simulation of convective systems we investigated during our tropical missions. The study by Chemel et al. (2009) is focussed on the strong Hector storm on 30 November 2005 over Tiwi Island which we probed with the Geophysica during SCOUT-O3. Several overshooting updraughts penetrating the tropopause are produced in the simulations during the mature stage of Hector. The penetration of rising towering cumulus clouds into the lower stratosphere maintains the entrainment of air at the interface between the UT and the LS. Vertical exchanges resulting from this entrainment process have a significant impact on the redistribution of atmospheric constituents within the UTLS region at the scale of the islands. In particular, a large amount of water is injected in the lower stratosphere. The fate of the ice particles as Hector develops drives the water vapour mixing ratio to saturation by sublimation of the injected ice particles, moistening the air in the LS, supported by our observations (Section 4.3) and confirming the results of box model calculations of Corti et al. (2007). The quantity of injected water by a single storm, however, is uncertain: Both models used in Chemel et al. (2009) yielded water entry values differing by more than an order of magnitude. Nevertheless, the moistening effect of such overshoots was identified unambiguously.

Fierli et al. (2011) simulated a convective system over Africa in comparison with our AMMA/SCOUT-O3 measurements. This study, however, is restricted to the TTL composition below the cold point. The authors found large redistribution of trace species including water along with these mesoscalic systems.

5 Ice clouds and saturation at the tropical tropopause

Ice clouds are a crucial phenomenon in the process of hydration and dehydration processes in the TTL. Their occurrence may be an indicator of ongoing dehydration – but also, as shown in Section 4.3, provide evidence for moistening if injected in dryer air masses. Hereby, their size or ice water content (IWC) plays a crucial role. Another key control parameter is the relative humidity with respect to ice RH_{ice} that determines whether the cloud particles will further grow or evaporate. In this Chapter, I present our observations of tropical cirrus and discuss their formation processes and their impact on the entry of water into the stratosphere.

5.1 Ice water content and hydration/dehydration potential of cirrus particles

5.1.1 Observation of specific cirrus

The most surprising finding during the APE-THESEO measurements over the Indian Ocean was the frequent occurrence (30% of observation time) of thin cirrus layer close to the cold point with large horizontal coverage of several thousands of square kilometres (Peter et al., 2003). These clouds have a vertical extend of only a few 100 m and very low ice water content (IWC), among the thinnest clouds ever observed so far and therefore named Ultrathin Tropical Tropopause Cirrus (UTTC). Figure 12 shows the measurement from the lidar perspective (measured from the Falcon aircraft flying below) and the in-situ measurements of the Geophysica. The occurrence and characteristics of these clouds was a paradox for us for a long time: How can an IWC corresponding to a fraction of only 1-5% of the ambient water be maintained over these large areas? Rapid growth or fast evaporation would be expected for such thin clouds. From the measurements (lowest panel in Figure 12, red line), we could exclude that they carry a larger amount of nitric acid – and our total water measurement showed slight enhancements whenever we crossed the cloud layer (lower panel in Figure 12, black line), corroborated by the measurements of particles (central panel in Figure 12). Thus the particles are identified as ice particles.

In Luo et al. (2003b) was shown that the UTTC are composed of ice in equilibrium and subject to a delicate stabilization mechanism between their sedimentation rate and the upwind velocity in that region. In another paper by Luo et al. (2003a), the dehydration potential of these thin clouds was investigated: The unique combination of high altitude and low number density makes UTTCs highly suited to serve as an effective drying agent during the last step of dehydration of air directly before troposphere-to-stratosphere exchange. In conclusion, UTTCs in a global average are likely to yield a lowering of 0.35 ppmv of H_2O in the air exchanged from the troposphere to the stratosphere.

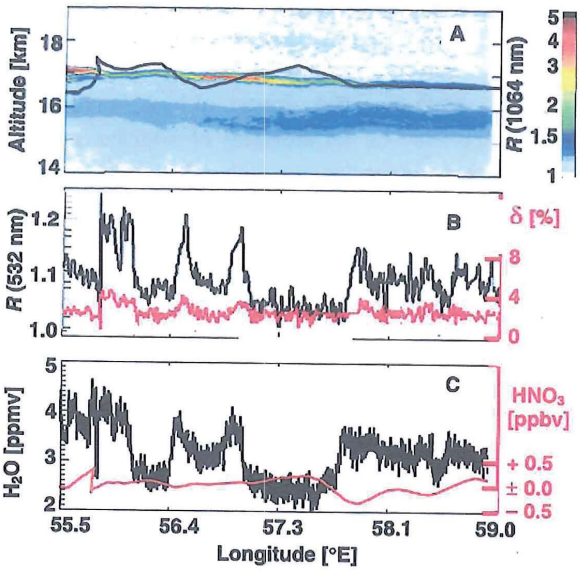

Figure 12: *Lidar backscatter ratio at of a 200–300 m thick UTTC at 17 km altitude observed onboard the Falcon on 27 Feb 1999. The Geophysica flight track is marked by black line. In situ measurements on board Geophysica of (B) backscatter ratio R (black curve) and volume depolarization d (red curve) and of (C) total water measured by FISH (black curve) and particulate nitric acid (red curve). (from Luo et al., 2003a).*

Santacesaria et al. (2003) investigate also a thin cirrus close to the tropopause during APE-THESEO, however with higher IWC derived from our FISH data than that of the UTTC discussed above. This cloud is located above a cumulonimbus (Cb) convective cluster. The brightness temperature calculated along backtrajectories suggests that the cirrus cloud has not been advected from other regions but has been generated locally. Furthermore, we found an extremely high, cold, and relatively humid tropopause in the region of the cirrus cloud. A possible mechanism of the cirrus formation is based on a net mesoscale transport of water vapour from altitudes above the Cb top (16 km) to the tropopause region around 18 km. This transport could be driven by the critical layer and turbulence induced by gravity waves generated by lower level Cb cluster activity. The data set also supports study by Teitelbaum et al. (1999) about mixing layers induced by gravity waves, but extending their conclusion by showing that absorbed gravity waves could also have a role into the formation of thin cirrus at the tropopause. The cirrus formation is thus a consequence of local activity and does not require tropopause penetrating Cbs. So, the proposed mechanism for high-altitude cirrus formation corroborates the paradigm of a tropical tropopause layer (TTL) several kilometres thick, which is decoupled from the convection-dominated lower troposphere (Fueglistaler et al., 2009, and references therein). A similar dehydration mechanism has been proposed to explain a dry air mass in the upper troposphere above a tropical cyclone during the same campaign (Cairo et al., 2008).

5.1.2 Climatology of the ice water content

In the following, I present a climatology of ice water content (IWC) derived from FISH data (Schiller et al., 2008). The data are obtained from the four tropical sites, complemented by data from mid latitudes (ENVISAT 2002; Cirrus 2003 and 2004 campaigns) and high latitudes (POLSTAR 1997 and 1998; EUPLEX/ENVISAT 2003 campaigns) using different aircraft. In total, 52 flights in cirrus are analysed. For a subset of 28 flights, the measurements are complemented by gas phase measurements of H_2O. For this subset, we derive IWC as the difference between the total water measurement H_2O_{tot} and the gas phase measurement H_2O_{gas}, divided by the enhancement factor E_{max}: $IWC = (H_2O_{tot}-H_2O_{gas})/E_{max}$ (Schiller et al., 2008; Krämer and Afchine, 2004). For the full data set, the ice water content is determined as the difference between the FISH total water measurement and the water vapour saturation mixing ratio, divided by the enhancement factor: $IWC = (H_2O_{tot}-H_2O_{sat}(T))/E_{max}$. Hereby, the saturation mixing ratio H_2O_{sat} is calculated from pressure and temperature measurement onboard the aircraft using the empirical equation by Marti and Mauersberger (1993). With this method, we neglect that cirrus clouds can exist in super- and subsaturated regions. However we will show in Section 5.2 that the assumption of RH_{ice} = 100% is a good approximation for the mean conditions in cirrus. Further, both approaches to calculate IWC yield almost the same fit functions for the mean, median and lower envelope or detection limit. This does not only confirm the validity of both approaches, but also demonstrates that the chosen subsets of data give similar results and are therefore representative samples of the atmosphere.

De Reus et al. (2009) determined the IWC independently from in-situ particle probes onboard the Geophysica during the SCOUT-O3 campaign. Comparison with the IWC derived from our total and gas-phase water measurements yielded a good agreement within the combined error bars of both methods.

Figure 13 shows the temperature dependence of the IWC for our complete data set. For each temperature, the IWC varies over several orders of magnitudes. However, the striking feature is the strong temperature dependence for the mean with decreasing IWC towards lower temperatures. Hereby, the tropical data yield those with lowest temperatures and IWC of the full data set down to 183 K, the mid-latitude data cover a range from 203 to 250 K, and the Arctic data from 198 to 250 K. As the largest drop in IWC occurs below 205 K, the tropical data are the key to understand the IWC-temperature dependence. Our data set therefore extends previous climatologies which were restricted to mid-latitudes (e.g. Wang and Sassen, 2002; Gayet et al., 2006).

We also determined fit functions for the mean, the median and envelopes of the data set which can be used as parameterisations in models. In order to account for the strong gradient toward low temperatures, we used functions of the type $10^{(a \cdot b^T+c)}$. The coefficients a, b and c are listed for the various fit functions in Schiller et al. (2008). Simpler functions as used by Wang and Sassen (2002) and Gayet et al. (2006) for mid-latitude data sets are not suited for extrapolation towards lower temperatures, as they would overestimate the IWC for these conditions. The mean and median functions for the complete climatology are also plotted in Figure 13. The fit function for the mean derived by Wang and Sassen (2002) is given in Figure 13 and agrees well in the respective temperature range. Also the climatological study for

tropical cirrus by McFarquhar and Heymsfield (1997) is broadly consistent with the observed drop in average IWC to lower temperatures; however this data set is restricted to temperatures down to 205 K only as their aircraft did not reach the cold point altitude.

In addition, we determined the frequency of occurrence of IWC (Schiller et al., Figure 6 therein). The core region, i.e. where the frequency of occurrence exceeds 5%, is a band of about one order of magnitude around the median and thus narrows the range of likely IWC for a temperature bin substantially.

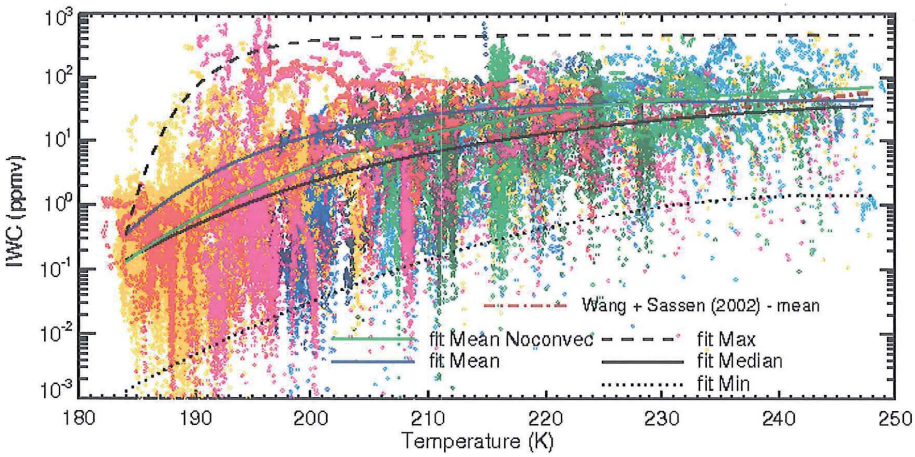

Figure 13: *Ice water content (IWC) of cirrus clouds versus temperature from all Arctic, midlatitude and tropical campaigns. Color codes denote the individual campaigns (yellow/red tropics; green mid latitudes; blue high latitudes). The solid black/blue/green lines are the fitted median/mean/mean (without convective events) of the full data set, the hatched line the fit of the maximum IWC, and the dotted line that of the minimum IWC, derived from 28 flights with gas-phase H_2O measurements available. (from Schiller et al., 2008)*

In Figure 14 those tropical flights are marked in red color which have been carried-out in or in the vicinity of deep convection, i.e. the APE-THESEO flight on March 9, 1999, the TroCCi-NOx flight on February 4, 2005, and the SCOUT-O3 flights on November 23, 29, and 30, 2005. On these days, convection up to the cold point tropopause or even higher transported ice particles and water into this very cold region (see Section 4.3). The highest IWC have been observed in the upper parts of the anvil or in overshooting turrets of these convective systems.

Besides regions of fresh deep convective events (blue data in Figure 14), also the upper envelope of the IWC of cirrus clouds is decreasing with decreasing temperature similar as the median and coincides almost with the upper limit of the core region with maximum frequency of occurrence. Maximum IWC values at 190 K are 1-2 ppmv and thus about one order of magnitude lower than at 210 K temperature. Deep convection occasionally transports ice particles with an IWC much higher than this upper envelope into the tropopause region. The observed IWC of 10-100 ppmv (or higher) in these events may exceed the climatological IWC distribution of the core belt by more than one order of magnitude. Thus we confirm with

independent evidence our previous findings from Section 4.3 that deep convection can transport substantial amounts of water into the upper TTL and even above the tropopause moistening its environment.

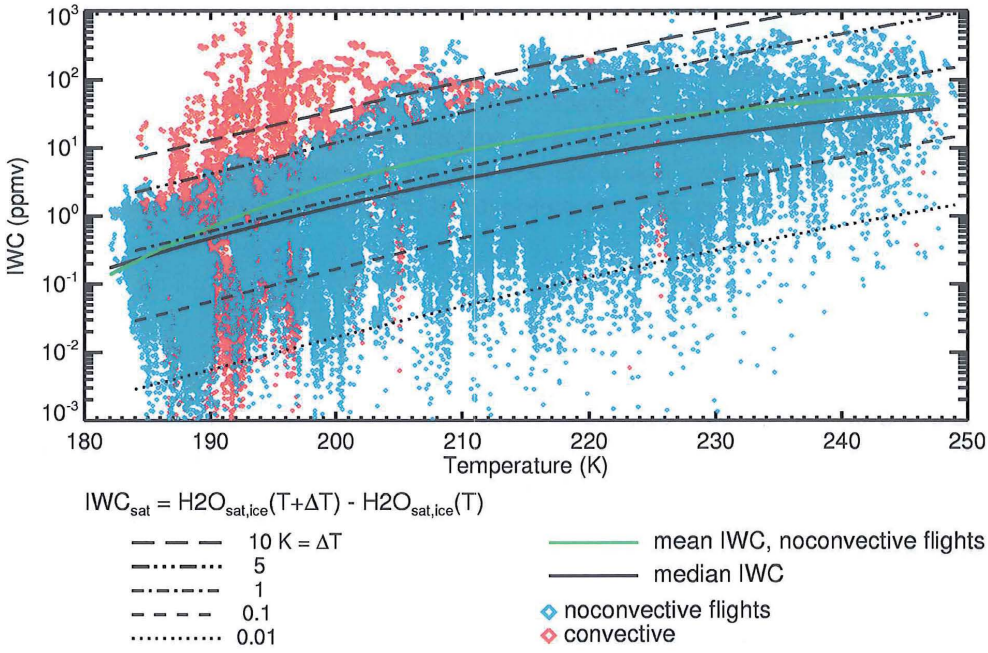

Figure 14: *Ice water content versus temperature as in Figure 13, but data observed during flights in the vicinity of deep convection are highlighted in red. Black lines represent IWC_{sat} for T+0.01K, T+0.1K, T+1K, T+5K and T+10K, respectively. (from Schiller et al., 2008)*

Now, we compare the temperature dependence of the IWC median with functions of the form $10^{a/T+b}$, the same type of formula as the approximated Clausius-Clapeyron equation which Marti and Mauersberger (1993) used to fit the ice saturation data. Using this formula, we calculate curves of ice water contents $IWC_{sat} = H_2O_{sat,ice}(T+dT) - H_2O_{sat,ice}(T)$, with dT = 0.01, 0.1, 1, 5 and 10 K, which are overlaid in Figure 14. IWC_{sat} can be regarded as the maximum IWC of a cirrus cloud at a cooling of dT when the cooling process starts at RH_{ice} = 100%. This very simplified approach however only describes the net effect of the cloud life cycle, as a real cirrus particle forms in a cooling process and then may sediment and evaporate in subsaturated environment. The IWC of convective cirrus cannot be described by the simple approximation derived from $H_2O_{sat,ice}$; these clouds are formed by freezing of warmer liquid clouds nucleated at lower altitudes, while the in-situ cirrus arise from deposition freezing which is correlated to $H_2O_{sat,ice}$. The mean of the IWC data (Figure 13) coincides best with IWC_{sat} at dT = 1 K for a large range of temperatures. In other words, on average the clouds are observed in air masses which have suffered a net cooling by approximately 1 K below the frost point temperature. On the one hand, the similarity of the temperature dependence of the measured mean IWC and the IWC_{sat} curves is not surprising since both phenomena are based on the same thermodynamical processes, the first one observed in the atmosphere and the latter one based on laboratory experiments. On the other hand, from the large vari-

ability of IWC occurring in the real atmosphere for a specific temperature and the range of potential supersaturation one can not a priori expect that the mean of our IWC data set is showing this similarity.

The decrease of IWC with temperature is also visible in the minimum and maximum values of IWC. IWC_{sat} calculated for temperatures 5 K above the frost point represents an upper envelope for those IWC data not impacted by fresh convection. This implies that cirrus build-up induced from cooling of about 5 K is an approximate upper limit in the TTL, except in a convective case. The lower limit of the core belt are a composite of cirrus particles which either have suffered a very moderate cooling (0.1 K or less) or have sedimented from above and are in a decaying stage.

5.2 Ice supersaturation and cirrus clouds

In a similar way as for the IWC, we derived a climatology of relative humidity over ice RH_{ice} as a function of temperature from our data sets (Krämer et al., 2009). However, hereby data of FLASH and an open-path diode laser spectrometer OJSTER are used as these instruments measure gas phase water. OJSTER was operated by my group during part of the mid-latitude measurements (Schlicht, 2006) which again complement the tropical data set for this climatology.

As explained in Section 2.3 and in more detail in Krämer et al. (2009), these data sets had to undergo a strict quality check in comparison with simultaneous FISH measurements. Uncorrected data yield striking results in terms of frequent unrealistic high supersaturations (Krämer et al., 2009), similar to those observations which impacted the rational of the article by Peter et al. (2006; see Section 1.3).

Our climatology again covers the complete relevant temperature range from 183 to 240 K. It exceeds therefore previous studies based on single campaign data, e.g. that of INCA (215-215 K; Ovarlez et al., 2002) and CRYSTAL-FACE (195-240 K, Gao et al., 2004). Again, our tropical data are essential for the extension to the lowest temperatures where highest supersaturations occur as expected from theory (Koop et al., 2000) and as discussed below.

In the following, we discriminate data measured under clear sky conditions and those measured inside clouds, based either on the simultaneous FISH data or – if available – by particle measurements. Figure 15 shows the frequency distribution of RH_{ice} binned in 1 K intervals from 193 to 240 K. In both panels, the homogeneous freezing threshold and water saturation are marked.

The clear sky data in the upper panel show RH_{ice} almost randomly distributed from zero to the homogeneous freezing threshold (Koop et al., 2000). Only very few data exceed this line and none the water saturation. Therefore the data set is well in accordance with theory, i.e. the majority of clear sky data is subsaturated, while in some cases supersaturation up to the freezing threshold may occur. The lower RH_{ice} limit is enveloped by the dashed line, representing a constant H_2O value of 1.5 ppmv., the minimum water mixing ratio observed in our data (see Figure 7). The highest frequency of occurrence are enclosed by the dashed lines

corresponding to 1.5 and 3.0 ppmv corresponding to typical mixing ratios near the tropical tropopause where most of our measurements were made.

In-cloud data of RH_{ice} are aligned around the RH_{ice} = 100% line (from 50% to the homogeneous freezing line, with very few exceptions). Highest frequencies of occurrence are at 100%. This behaviour can be expected for a mixture of cirrus probed in the three stages, i.e. equilibrium, growth and evaporation. The frequency of higher supersaturations increases towards lowest temperatures and the distribution becomes more scattered, which could be explained by longer relaxation times under these conditions (see below). Our RH_{ice} values are generally lower than those obtained with the HWV/JLH data (e.g. Gao et al., 2006) who measured an average occurrence of RH_{ice} of 110-130% inside clouds and peak values exceeding significantly the freezing and water thresholds. These discrepancies are likely caused by systematic differences of the instruments used (see Chapter 2). The more canonical results we obtained could be an indication for the validity of our data set.

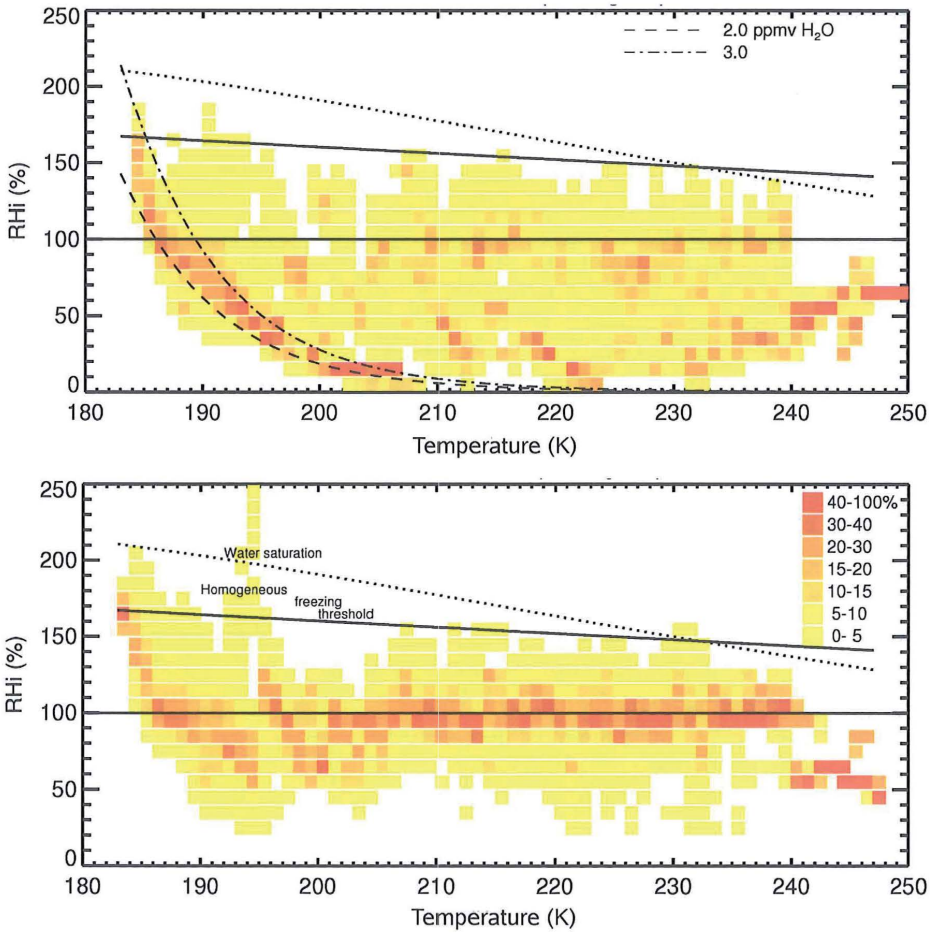

Figure 15: *Occurrence frequency of RH_{ice} vs. temperature; solid line: homogeneous freezing threshold, dotted line: water saturation line; data are sorted in 1K temperature bins. Top panel: clear sky data; bottom panel: inside cloud data. (from Krämer et al., 2009)*

To further explain the pattern of RH_{ice} inside cirrus, in particular observed persistently high supersaturions, we discuss the dynamical equilibrium, i.e. when the mean size of the particles R_{ice}, the ice particle number N_{ice} and the vertical velocity v_z (or cooling rate) are nearly constant. Korolev and Mazin (2003) describe the supersaturation at dynamical equilibrium as $RH = v_z/N_{ice}R_{ice} \cdot a_0/b_i - b_i^*/b_i$ with coefficients a_0, b_i and b_i^* dependent on temperature, pressure etc.. The relaxation time to reach from an initial in-cloud supersaturation the equilibrium is given as $\tau = 1 / (a_0 v_z + (b_i+b_i^*)N_{ice}R_{ice})$. Highest supersaturations can therefore be reached at high v_z and low $N_{ice} \cdot R_{ice}$, and they can be maintained longest for low v_z and low $N_{ice} \cdot R_{ice}$. For a more detailed discussion see Krämer et al. (2009).

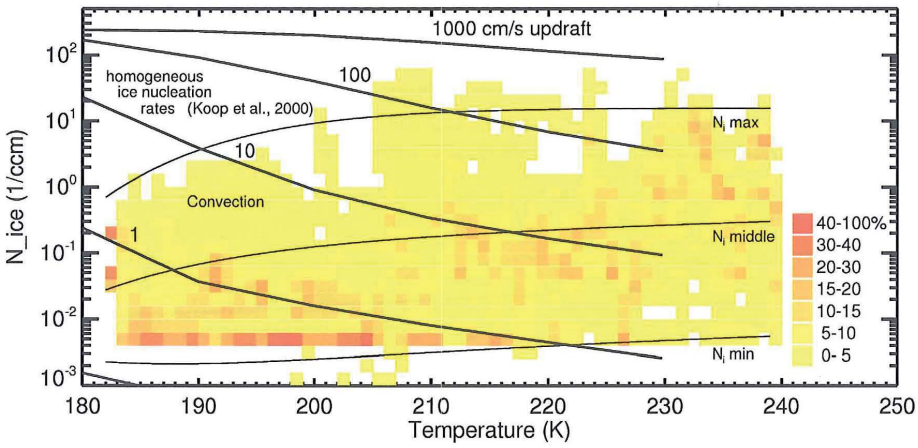

Figure 16: *Frequencies of occurrence of ice crystal numbers N_{ice} (top panel) and sizes R_{ice} (bottom panel) vs. temperature (same dataset as Figure 15; thin solid lines: minimum, middle and maximum N_{ice} and R_{ice}; thick solid lines in top panel: ice crystal numbers calculated for homogeneous freezing at different updraft velocities). (from Krämer et al., 2009)*

Frequency distribution of N_{ice} and R_{ice} have been derived from the same 20 Geophysica flights as in Figure 15 using in situ particle measurements (de Reus et al., 2009) and are displayed in Figure 16 (Krämer et al., 2009). The minimum/middle/maximum N_{ice} and R_{ice} fit functions are overlaid as thin lines. The number of ice crystals that would form homogeneously for different v_z is shown as thick lines in the upper panel of Figure 16. They are calculated by a simple box model (see Krämer et al., 2009). The most obvious feature is that the simulated ice crystal numbers formed by homogeneous freezing increase with decreasing temperature for each v_z, while the most frequently observed N_{ice} decreases, confirming and extending the observations of Gayet et al. (2006) in the temperature range 210–260K.

As mentioned above, for low temperatures the supersaturation pattern becomes spread, implying that the water vapour relaxation times are longer here. Such long relaxation times can be caused by the slower water vapour diffusion in that temperature range, but more important, low N_{ice} and/or high v_z. As Figure 16 shows, at temperatures below 205 K lowest N_{ice} are indeed most frequent and thus becomes the dominant parameter to explain high supersaturations. The calculation of N_{ice} for these conditions assuming homogeneous nucleation (thick lines) implies that such low numbers can occur only at very low v_z. As alternative explanations, we propose either heterogeneous nucleation or nucleation suppression at very

low temperatures. In summary, the high supersaturations at low temperatures – often persistently measured – are well in accordance with our known nucleation theory and are accompanied by very low N_{ice}. The question remains, however, to explain these low N_{ice}, and several studies have been done recently to find potential nucleation suppressing mechanisms (e.g. Zobrist et al., 2008; Murray et al., 2010).

5.3 Does HNO_3 matter?

Nitric acid (HNO_3) as a condensable gas is subject of many cloud investigations primarily to study the redistribution of HNO_3 and its impact on photochemistry in the upper troposphere (e.g. von Hobe et al., 2011). We use our IWC data together with measurements of nitrogen oxide species to determine the HNO_3 content in cirrus ice (Voigt et al., 2006; Voigt et al., 2007; Krämer et al., 2008). Hereby, the tropical data from SCOUT-O3 and additional data from CRYSTAL-FACE (Popp et al., 2007) extend the temperature interval down to 185 K. The HNO_3/H_2O mole fraction in ice is found to increase steadily with decreasing temperature (Voigt et al., 2006; Krämer et al., 2009). Figure 17 shows that in a climatological view, the HNO_3 content increases with decreasing temperature in the range 240 – 200 K. For colder ice clouds, the average HNO_3 content again decreases. At higher temperatures, less efficient HNO_3 uptake limits the HNO_3 content in cirrus ice, while at low temperatures small IWC (see Section 5.1.2) permit only little HNO_3 in ice, thus causing the convexly shaped average HNO_3 content curve. The highest HNO_3 content is expected in tropical ice clouds with very large IWC, especially at temperatures between 190 and 210 K.

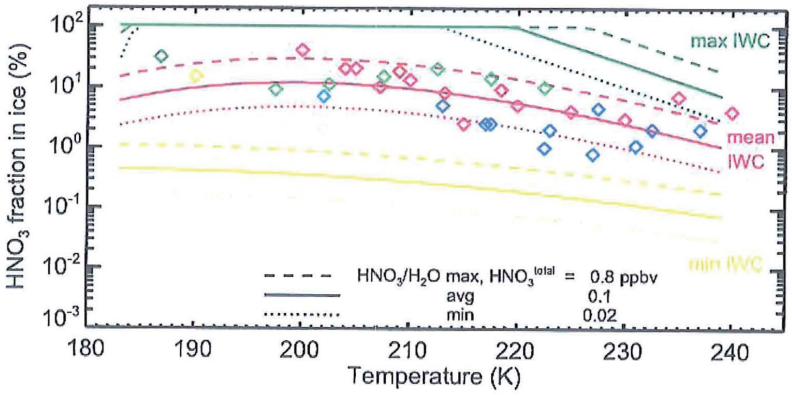

Figure 17: *Fraction of total HNO_3 in cirrus ice; diamonds: average field observations; lines denote several max/min scenarios discussed in Krämer et al. (2008). (from Krämer et al., 2008).*

Pure nitric acid trihydrate (NAT) clouds are observed frequently in the polar stratosphere and play a key role in chemistry impacting the ozone layer (e.g. Solomon et al., 1988). Near the tropical tropopause, however, NAT is stable at conditions about 2 K above the ice frostpoint T_{ice}, hence there exists only a small temperature window for the detection of pure NAT clouds (Popp et al., 2007). During our tropical missions, NAT particles were detected during one flight over Africa (Voigt et al., 2008). The NAT particle layer on that day was repeatedly ob-

served at altitudes between 15.1 and 17.5 km over extended areas. Satellite observations suggest that the NAT particles could have nucleated on ice fed by convective activity. Model calculations imply that such particles might build a larger area and occur over longer periods; however, our observations were restricted to this single event.

As the abundance of HNO_3 near the tropical tropopause is about three orders of magnitudes lower than that of H_2O, its role for the water budget and cirrus composition is negligible. Pure NAT clouds seem to be rare here. Some studies, however, propose that the uptake of HNO_3 on ice clouds – even in small amounts – may alter the water vapour pressure over of the ice crystals and therefore could be a reason for observed supersaturations (e.g. Gao et al., 2004). Such hypotheses still need confirmation by controlled laboratory experiments. Further, as shown in Section 5.2, our data set agrees with our current theoretical understanding and does not imply such additional processes.

6 Conclusions and outlook

In the Introduction, I focussed the understanding of the tropical water entry into the stratosphere on two fundamental questions:

Along which pathways is water transported and freeze-dried on its way into the stratosphere? Which conditions do control the freeze-drying process at the tropical tropopause?

To give answers to these questions in Chapters 4 and 5, respectively, we measured and used a comprehensive data set of water during four aircraft campaigns in the tropics. The missions were carried out in different tropical regions during various seasons, thus providing complementary information and catching different phenomena characteristic for the location. The main conclusions we derive from the individual studies are:

Data quality. The answers to our key questions critically depend on the quality of water measurements. Systematic differences have been identified between different instruments. Therefore the calibration procedure of our hygrometers has been revisited and the data set has been revised where necessary. We therefore are confident that we present one of the most reliable data set of water down to the critical ppmv range. An assessment of such a statement however requires the cooperation in the international community as foreseen in the next SPARC Water Vapour Assessment as outlined in Schiller et al., 2008. In this work, I described first the accuracy of our data set and then draw scientific conclusions. But from scientific findings, its worth to cycle back to the data quality question: The sound conclusions in accordance with accepted theory may be used as a proof on the validity of the data set. So the single results summarised in the following can be composed – together with the quality discussion – to a closure study of this complex science theme.

Competing hydration and dehydration in the TTL. The tropical water vapour entry into the stratosphere is found to be a highly complex interplay between freeze-drying in the coldest regions of the TTL and fresh supply of water by convection or by mixing with tropospheric air. Based on our studies, the 420 K isentrope appears to be the transition between a regionally controlled regime and a zonally well mixed compartment at higher altitudes. This is a quantitative confirmation of the TTL concept discussed in Fueglistaler et al. (2009). It marks the highest altitude of direct impact of overshooting convection. Further, recent condensation and sedimentation of particles may have altered the composition below 420 K leading to regional deviations from the zonal mean. Though an interannual variability of the TTL parameters has been observed to propagate further up and is visible in the different tape recorder signals, the local and regional variability in the TTL becomes smeared out above 420 K. Different types of models simulated the various underlying processes and successfully used our data set for their validation.

Large-scale advection. Trajectory-based reconstruction of water vapour, initialised with climatological HALOE data, yields a remarkable agreement with our in-situ observations above the tropopause for the different regions and seasons studied. Therefore the Lagrangian saturation history on time scales of hours to 1 month appears to be appropriate and sufficient to describe the average H_2O distribution at the cold point tropopause and in the first kilometres above. So, our results confirm previous findings from similar Lagrangian studies (e.g. Fue-

glistaler et al., 2005; Fueglistaler and Haynes, 2005), however now demonstrated with a data set of much finer scales in time and space and thereby covering different tropical regions and seasons. Jensen and Pfister (2004) tested with a more sophisticated Lagrangian ice cloud model the sensitivity of the stratospheric vapour entry on cloud properties and their dependence on wave perturbations and other parameters. While cloud frequency and distribution was very sensitive on these parameters, they also concluded that final water vapour mixing ratios are primarily controlled by the minimum temperatures encountered. Our study confirms these studies and thereby the preceding ideas of Holton and Gettelman (2001) with new experimental evidence that, despite the complex interplay of various processes leading to a highly variable water distribution in the tropics, stratospheric water vapour entry is primarily controlled by the coldest regions in the TTL, in which the air is freeze-dried to its final set point during its way into the stratosphere.

Moistening by deep convection. The main outflow of convection below the cold point as well as frequently observed local overshoots into the stratosphere have been unequivocally identified to moisten their environment, in contrast to earlier hypotheses by Danielsen (1993 and Sherwood and Dessler (2002). Below the tropopause, our measurements show significantly higher H_2O mixing ratios than inferred from the backtrajectory history which does not consider recent individual convective systems. However, no significant remnants of this high water released in the lower TTL can be found above the cold point anymore as this additional water is removed on its way through the cold point. We found layers of enhanced water vapour above the cold point which could be traced to direct injection by overshooting turrets. These irreversible injections of H_2O up to 420 K were observed to be isolated and thus highly localised, i.e. with horizontal extensions on the order of 50 km. Even if an estimate of the amount of water injected in such a single event is possible (Chemel et al., 2009), an upscaling of its global impact on the stratospheric water vapour budget might be possible only with large uncertainties, based on global observations of the frequency of such events (Gettelman et al., 2002; Liu and Zipser, 2005). The comparison of our data with the HALOE-initialised reconstruction of H_2O however gives a hint on the maximum possible impact of overshoots on the stratospheric water vapour budget. For SCOUT-O3 and to a lesser extent also for TroCCiNOx conditions, additional water injected above the cold point can still be freeze-dried to the low mean values there. The comparison of the AMMA/SCOUT-O3 data with the climatological HALOE profile might suggest enhanced water vapour abundance over Africa. Most likely, the observed discrepancy however reflects the formerly identified low bias of HALOE compared to FISH data. Zonal asymmetries and interannual variability could contribute an uncertainty on the order of 10%. In summary, an impact of deep convection to the stratospheric water entry of more than 10% appears to be unlikely from our studies.

Cirrus clouds. We observed a large spectrum of cirrus clouds down to very thin ones occurring at lowest temperatures. Their ice water content and other parameters measured are indicative for their formation process and their potential to hydrate or dehydrate the air on its way to the stratosphere. Thin cloud layers with lowest IWC extended and large horizontal coverage have been identified to be the final step setting the water entry in the tropical tropopause region. At low temperatures, IWC significantly higher than the climatological mean,

could be attributed to overshooting cloud particles and corroborate the aforementioned findings that the stratosphere can be locally moistened by these injections.

Supersaturation. This phenomenon postulated from theory and identified in several laboratory and atmospheric measurements before, is apparent in our tropical data set as well. In contrast to a few findings of other groups, our data set however confirms the classical theory combined with some recent findings, both for cloud and clear-sky observations; the reason for these differing conclusions can be primarily traced to the identified systematic discrepancies of the instruments. Including standard supersaturations, our water reconstruction showed only a weak sensitivity for the water vapour entry. This result is consistent with the previous study by Jensen and Pfister (2004).

Where do we go? Our understanding how water vapour is transported into the stratosphere and herby freeze-dried in the tropics has been substantially increased by the experimental and model studies during the last decade. The combination of new aircraft and balloon experiments, new satellite data sets and model studies on different scales supported by dedicated laboratory studies enabled this progress. However, the following challenges remain our tasks for the coming years:

We have to resolve the discrepancies in different data sets in the community, as they still allow for different interpretation of individual processes. This task has to be continued in an open international cooperation of the key experimental groups in hygrometry and to be accompanied by theory teams, as planned in the upcoming SPARC Water Vapour Assessment.

The exchange of air between tropics and subtropics is still a large uncertainty to assess the global entry of water into the stratosphere, as a by-pass of the standard pathways in the tropics seems to be possible. Also the range of the tropical entry region at its edges needs better quantification. The complex of the Asian monsoon has been identified in several studies to be the key unknown in this respect and will therefore certainly be the target region for upcoming aircraft experiments.

We identified and characterised several local processes, in particular overshooting convection, that potentially influence the troposphere-to-stratosphere exchange also on larger scales. Though our studies did not confirm a major global impact, a thorough upscaling of these phenomena and their inclusion in operational and science models is a challenging task for the future.

Temperature was identified to be the driving parameter for the tropical water vapour entry in our and other studies. Future changes of stratospheric water will therefore critically depend on changes in tropical temperature in the tropopause region. Its determination in current weather and chemistry-climate models is still a challenge, as feedback with water and clouds as well as radiative processes still has large uncertainties. Therefore, measurements of water vapour in the tropical tropause region will remain also in the future a key component on our way towards a prediction of stratospheric composition and climate.

Acknowledgements

Martin Riese and Ralph Koppmann encouraged me to compile this habilitation thesis and were always open for discussions. Martin Riese supported me in the last decade to carry out the scientific programme that is described here with helpful scientific and programmatic advice. My interest in this research topic and the experimental basis was initiated already in ealier years when working with Dieter Ehhalt, Ulrich Schmidt, Dieter Kley and Danny McKenna.

Nicole Spelten, Armin Afchine, Vicheith Tan, Axel Schönfeld, Reimar Bauer and Jochen Barthel are the team of technicians and engineers, who made the experimental programme with FISH successful, despite the 'instrument-unfriendly' environment in the tropics.

My colleagues in Jülich, who shared their ideas about the data with me for the publications: Martina Krämer, Paul Konopka, Jens-Uwe Grooß, Fred Stroh, Susanne Rohs, Rolf Müller, Marc von Hobe. And the students in my group, who provided major results within their Diploma and PhD thesis to this research topic: Jürgen Beuermann, Oliver Bujok, Jessica Meyer, Felix Plöger, Fábio Silva dos Santos, Stefanie Schlicht and Martin Zöger.

Planning of the aircraft campaigns, from the entire project to individual flight patterns, as well as discussing strategies and results was the task of a coordinating groups, including: Dominik Brunner, Francesco Cairo, Neil Harris, Stephan Fueglistaler, Thomas Peter, John Pyle, Rob MacKenzie, Jean-Pierre Pommereau, Hans Schlager, Ulrich Schumann, Leopoldo Stefanutti, and Geraint Vaughan.

Operation of the Geophysica aircraft under difficult conditions and in remote countries was a challenge, but successfully carried out due to the hard work of Stefano Balestri, Heinz Finkenzeller, Rolf Maser, Harald Franke, Gennady Belyaev, Slava Khattatov, Oleg Shepetkov, Oleg Kononenko, and staff of the Myasishchev Design Bureau and DLR flight department.

No FISH without FLASH: Nicolay Sitnikov and Vladimir Yushkov are my most important cooperation partners for water vapour measurements from the Geopyhsica. Individual scientific studies exploiting the data were carried out with Stephan Borrmann, Thierry Corti, Marian de Reus, Federico Fierli, Beiping Luo, Peter Spichtinger, Christiane Voigt and with many colleagues mentioned above.

The AquaVIT laboratory experiment was a cooperation with David Fahey, Rushan Gao, Ottmar Möhler, Harald Saathoff, Volker Ebert, Elliot Weinstock, Sergey Khaykin, Holger Vömel, Robert Herman and Serhey Khaykin.

It was and is a pleasure to work with these enthusiastic colleagues. I thank all of them for their help, advice and their contributions to the results of this habilitation thesis.

The experiments were supported by several projects: EU EVK2-CT-2001-00122 (TroCCiNOx), EU GOCE-CT-2004-505390 (SCOUT-O3), INSU and Geophysica EEIG (AMMA), BMBF 01LA9829 (APE-THESEO), KIT and SPARC (AquaVIT).

Abbreviations and acronyms

AIDA	Aerosols, Interactions and Dynamics in the Atmosphere
AMMA	African Monsoon Multidisciplinary Analysis
APE-THESEO	Airborne Platform for Experiments – Third European Stratospheric Experiment on Ozone
APicT	AIDA-PCI-in-cloud-TDL
AquaVIT	Water Validation Intercomparison and Tests
CFH	Cryogenic Frostpoit Hygrometer
CLaMS	Chemical Lagrangian Model of the Stratosphere
CRISTA	Cryogenic Infrared Spectrometers and Telescopes for the Atmosphere
CRYSTAL-FACE	The Cirrus Regional Study of Tropical Anvils and Cirrus Layers – Florida Area Cirrus Experiment
DIAL	Differential Absorption Lidar
EUPLEX	European Polar stratospheric cloud and Lee wave Experiment
FISH	Fast In-situ Stratospheric Hygrometer
FLASH	Fluorescent Airborne Stratospheric Hygrometer
HALOE/UARS	Halogen Occultation Experiment / Upper Atmosphere Research Satellite
IWC	Ice Water Content
ILAS/ADEOS	Improved Limb Atmospheric Spectrometer / Advanced Earth Observation Satellite
JLH	JPL Laser Hygrometer
LACM	Lagrangian air-parcel cirrus model
MIPAS/ENVISAT	Michelson Interferometer for Passive Atmospheric Sounding / Environmental Satellite
MLS/AURA	Microwave Limb Sounder / ('breeze')
NAT	Nictric Acid Tryhydrate
NPL	National Physical Laboratory
OJSTER	Open-path Jülich Stratospheric TDL Experiment
POAM	Polar Ozone and Aerosol Measurement
POLSTAR	Polar Stratospheric Aerosol Experiment
PSC	Polar Stratospheric Cloud
PTB	Physikalisch-Technische Bundesanstalt
SCOUT-O3	Stratospheric-Climate Links with Emphasis on the Upper Troposphere and Lower Stratosphere
SOWER	Soundings of Ozone and Water in the Equatorial Region
STEP-Tropical	The tropical experiment of the Stratosphere-Troposphere Exchange Project
TroCCiNOx	Tropical Convection, Cirrus and Nitrogen Oxide experiment
TTL	Tropical Transition Layer
UTLS	Upper Troposphere / Lower Stratosphere
UTTC	Ultrathin Tropical Tropopause Cirrus

References

*** Key publication re-printed in the Appendix
** Additional relevant publications of C. Schiller as (co)author
* PhD or Diploma thesis supervised by C. Schiller

*Beuermann, J., Einfluss von Transportprozessen auf die Wasserdampfverteilung in der Tropopausenregion, PhD Thesis Univ. Bonn, 2001.

**Brunner, D., P. Siegmund, P. T. May, L. Chappel, C. Schiller, R. Müller, T. Peter, S. Fueglistaler, A. R. MacKenzie, A. Fix, H. Schlager, G. Allen, A. M. Fjaeraa, M. Streibel, N. R. P. Harris, Overview and meteorological context of the SCOUT-O3 aircraft measurement campaign in Darwin, Australia, Nov-Dec 2005, Atmos. Chem. Phys., 9, 93-117, 2009.

**Cairo, F., C. Buontempo, A. R. MacKenzie, C. Schiller, M. Volk, A. Adriani, V. Mitev, R. Matthey, G. Di Donfrancesco, A. Oulanovsky, F. Ravegnani, S. Rudakov, V. Yushkov, M. Snels, C. Cagnazzo and L. Stefanutti, Morphology of the tropopause layer and lower stratosphere above a tropical cyclone: A case study on cyclone Davina (1999), Atmos. Chem. Phys., 8, 3411-3426, 2008.

**Cairo, F., J. P. Pommereau, K. S. Law, H. Schlager, A. Garnier, F. Fierli, M. Ern, M. Streibel, S. Arabas, S., Borrmann, J. J. Berthelier, C. Blom, T. Christensen, F. D'Amato, G. Di Donfrancesco, T. Deshler, A. Diedhiou, G. Durry, O. Engelsen, F. Goutail, N. Harris, S. Khaykin, A. Kylling, P. Konopka, T. Lebel, X., Liu, R. MacKenzie, J. Nielsen, N. Sitnikov, A. Oulanowski, D. Parker, J. Pelon, J. Polcher, J. Pyle, F., Ravegnani, E. Riviere, E. D. Robinson, T. Röckmann, C. Schiller, F. Simoes, L. Stefanutti, F. Stroh, L. Some, P. Siegmund, N. Sitnikov, J. P. Vernier, C. M. Volk, C. Voigt, M. von Hobe, S. Viciani, and V. Yushkov, An introduction to the SCOUT-O3-AMMA stratospheric aircraft, balloons and sondes campaign in West Africa, August 2006: rationale and roadmap, Atmos. Chem. Phys., 10, 2237-2256, 2010.

Chaboureau, J. P., et al., A numerical study of tropical cross-tropopause transport by convective overshoots, Atmos. Chem. Phys., 7, 1731-1740, 2007.

Corti, T., B. P. Luo, T. Peter, H. Vömel, and Q. Fu, Mean radiative energy balance and vertical mass fluxes in the equatorial upper troposphere and lower stratosphere, Geophys. Res. Lett., 32, L06802, doi:10.1029/2004GL021889, 2005.

***Corti, T., B. P. Luo, M. deReus, D. Brunner, F. Cairo, M. J. Mahoney, G. Matucci, R. Matthey, V. Mitev, F. H. dos Santos, C. Schiller, G. Shur, N. M. Sitnikov, N. Spelten, H. J. Vössing, S. Borrmann, and T. Peter, Unprecedented evidence for overshooting convection hydrating the tropical stratosphere, Geophys. Res. Lett., 35, L10810, doi:10.1029/2008GL033641, 2008.

**Chemel, C., M. R. Russo, J. A. Pyle, R. J. Sokhi, C. Schiller, Quantifying the imprint of a severe Hector thunderstorm during ACTIVE/SCOUT-O3 onto the water content in the upper troposphere/lower stratosphere, Monthly Weath. Rev., 137, 2493-2514, doi:101175/2008MWR2666.1, 2009.

Danielsen, E. F., In situ evidence of rapid, vertical, irreversible transport of lower tropospheric air into the lower tropical stratosphere by convective cloud turrets and by larger-scale upwelling in tropical cyclones, J. Geophys. Res., 98, 8665-8681, 1993.

**de Reus, M., S. Borrmann, A. J. Heymsfield, R. Weigel, C. Schiller, V. Mitev, W. Frey, D. Kunkel, A. Kürten, J. Curtius, N. M. Sitnikov, A. Ulanovsky, and F. Ravegnani, Evidence for ice particles in the tropical stratosphere from in-situ measurements, Atmos. Chem. Phys., 9, 6775-6792, 2009.

Dethof, A., Aspects of modelling and assimilation for the stratosphere at ECMWF, available via: www.atmosp.physics.utoronto.ca/SPARC/News21/21_Dethof.html, SPARC newsletter 21, 2003.

Dlugokencky, E. J., S. Houweling, L. Bruhwiler, K. A. Masarie, P. M. Lang, J. B. Miller, and P. P. Tans, Atmospheric methane levels off: Temporary pause or a new steady-state?, Geophys. Res. Lett., 30, 1992, doi:10.1029/2003GL018126, 2003.

Dvortsov, V. L., and S. Solomon, Response of the stratospheric temperatures and ozone to past and future increases in stratospheric humidity, J. Geophys. Res., 106, 7505- 7514, 2001.

Ebert, V., Teichert, H., Giesemann, C., Saathoff, H., and Schurath, U.: Fibre-coupled in-situ laser absorption spectrometer for the selective detection of water vapour traces down to the ppb-level, Technisches Messen, 72, 23–30, 2005.

**Engel, A., C. Schiller, U. Schmidt, R. Borchers, H. Ovarlez, J. Ovarlez, The total hydrogen budget in the Arctic winter stratosphere during EASOE, J. Geophys. Res., 101, 14495-14503, 1996.

Fahey, D. W., R. S. Gao, O. Möhler, Summary of the AquaVIT Water Vapor Intercomparison: Static Experiments, available at: https://aquavit.icg.kfa-juelich.de/AquaVit/, 2009.

**Fierli, F., E. Orlandi, K. S. Law, C. Cagnazzo, S. Borrmann, F. Cairo, C. Schiller, F. Ravegnani, and M. Volk, Impact of deep convection in the tropical tropopause layer in West Africa: in-situ observations and mesoscale modelling, Atmos. Chem. Phys., 11, 201-214, 2010.

Forster, P. M., and K. P. Shine, Assessing the climate impact of trends in stratospheric water vapor, Geophys. Res. Lett., 29(6), 1086, doi:10.1029/2001GL013909, 2002.

Feck, T., J.-U. Grooß, M. Riese, Sensitivity of Arctic ozone loss to stratospheric H_2O, Geophys. Res. Lett., 35, L01803, doi:10.1029/2007GL031334, 2008.

Fueglistaler, S., M. Bonazzola, P. H. Haynes, and T. Peter, Stratospheric water vapour predicted from the Lagrangian temperature history of air entering the stratosphere in the tropics, J. Geophys. Res., 110, D08017, doi: 10.1029/2004JD005516, 2005.

Fueglistaler, S., and P. H. Haynes, Control of interannual and longer-term variability of stratospheric water vapor, J. Geophys. Res., 110, D24108, doi:10.1029/2006JD007273, 2005.

Fueglistaler, S., A. E. Dessler, T. J. Dunkerton, I. Folkins, Q. Fu, and P. W. Mote, Tropical tropopause layer, Rev. Geophys., 47, RG1004, doi:10.1029/2008RG000267, 2009.

Gao, R. S., P. J. Popp, D. W. Fahey, T. P. Marcy, R. L. Herman, E. M. Weinstock, D. G. Baumgardner, T. J. Garrett, K. H. Rosenlof, T. L. Thompson, P. T. Bui, B. A. Ridley, S. C. Wofsy, O. B. Toon, M. A. Tolbert, B. Kärcher, Th. Peter, P. K. Hudson, A. J. Weinheimer, A. J. Heymsfield, Evidence That Nitric Acid Increases Relative Humidity in Low-Temperature Cirrus Clouds, *Science,* 303. 516-520, doi:10.1126/science.1091255, 2004.

Gayet, J.-F., V. Shcherbakov, H. Mannstein, A. Minikin, U. Schumann, J. Ström, A. Petzold, J. Ovarlez, and F. Immler, Microphysical and optical properties of mid-latitude cirrus clouds observed in the southern hemisphere during INCA, Q. J. Roy. Met, 132, Part B, No. 621, 2721-2750, 2006.

Gettelman, A., M. L. Salby, and F. Sassi, Distribution and influence of convection in the tropical tropopause region, J. Geophys. Res., 107, doi:10.1029/2001JD001048, 2002.

Grooß, J.-U., and J. M. Russell III, Technical note: A stratospheric climatology for O_3, H_2O, CH_4, NO_x, HCL and HF derived from HALOE measurements, Atmos. Chem. Phys., 5, 2797-2807, 2005.

Grosvenor, D. P., T. W. Choularton, H. Coe, and G. Held, A study of the effect of overshooting deep convection on the water content in the TTL and lower stratosphere from cloud resolving model simulations, Atmos. Chem. Phys., 7, 4977-5002, 2007.

Holton, J. R., and A. Gettelman, Horizontal transport and the dehydration of the stratosphere, Geophys. Res. Lett., 28, 2799-2802, 2001.

Horseman, A. M., A. R. MacKenzie, M. P. Chipperfield, Tracers and traceability: implementing the cirrus parameterisation from LACM in the TOMCAT/SLIMCAT chemistry transport model as an example of the application of quality assurance to legacy models, Geosci. Model Dev., 3, 189–203, 2010.

Hurst, D. F., S. J. Oltmans, H. Vömel, K. H. Rosenlof, S. M. Davis, E. A. Ray, E. G. Hall, and A. F. Jordan, Stratospheric water vapour trends over Boulder, Colorado: Analysis of the 30 year Boulder record, J. Geophys. Res., 116, D02306, doi:10.1029/2010JD015065, 2011.

IPCC, Climate Change 2007: The physical science basis, Cambridge Univ. Press, Cambridge and New York, 2007.

James R., M. Bonazzola, B. Legras, K. Surbled, S. Fueglistaler, Water vapor transport and dehydration above convective outflow during Asian monsoon, Geophys. Res. Lett., 35, L20810, doi:10.1029/2008GL035441, 2008.

Jensen, E., and L. Pfister, Transport and freeze-drying in the tropical tropopause layer, J. Geophys. Res., 109, D02207, doi: 10.1029/2003JD004022, 2004.

Jensen, E., J. Smith, L. Pfister, J. Pittman, E. weistock, D. Sayres, R. Herman, R. Troy, K. Rosenlof, T. Thomson, A. Fridlin, P. Hudson, D. Czczo, A. Heymsfield, C. Schmitt, J. Wilson: Ice supersaturations exceeding 100% at the cold tropical tropopause: implications for cirrus formation and dehydration, Atmos. Chem. Phys., 5, 851-862, 2005.

Jensen, E. J., A. S. Ackerman, and J. A. Smith, Can overshooting convection dehydrate the tropical tropopause layer? J. Geophys. Res., 112, D11209, doi:10.1029/2006JD007943, 2007.

Jones, A., J. Urban, D. P. Murtagh, P. Eriksson, S. Brohede, C. Haley, D. Degenstein, A. Bourassa, C. von Savigny, T. Sonkaew, A. Rozanov, H. Bovensmann, J. Burrows, Evolution of stratospheric ozone and water vapour time series studied with satellite measurements, Atmos. Chem. Phys., 9, 6055-6075, 2009.

**Kanzawa, H. C. Schiller, J. Ovarlez, C. Camy-Peyret, P. Jesek, H. Oelhaf, M. Stowasser, W. A. Traub, K. W. Jucks, D. G. Johnson, G. C. Toon, B. Sen, J.-F. Blavier, J. Park, G. E. Bodeker, L. L. Pan, T. Sugita, H. Nakajima, T. Yokota, M. Suzuki, M. Shiotani, Y. Sasano, Validation and data characteristics of water vapor profiles observed by the Improved Limb Atmospheric Spectrometer (ILAS) and processed with Version 5.20 algorithm, J. Geophys. Res., 107, D24, 8217, 2001JD000881, 2002.

Kelly, K. K., M. H. Proffitt, K. R. Chan, M. Loewenstein, J. R. Podolske, S. E. Strahan, J. C. Wilson, and D. Kley, Water vapour and cloud water measurements over Darwin during the STEP 1987 tropical mission, J. Geophys. Res., 98, 8713-8723, 1993.

Khaykin, S., J.-P. Pommereau, L. Korshunov, V. Yushkov, J. Nielsen, N. Larsen, T. Christensen, A. Garnier, A. Lukyanov, E. Williams, Hydration of the lower stratosphere by ice crystal geysers over land convective systems, Atmos. Chem. Phys., 9, 2275-2287, 2009.

**Kiemle, C., M. Wirth, A. Fix, G. Ehret, U. Schumann, T. Gardiner, C. Schiller, N. Sitnikov, G. Stiller, First Airborne Water Vapor Lidar Measurements in the Tropical Upper Troposphere and Mid-latitudes Lower Stratosphere: Accuracy Evaluation and Intercomparisons with Other Instruments, Atmos. Chem. Phys., 8, 5245-5261 (2008).

Kley, D., A. L. Schmeltekopf, K. Kelly, R. H. Winkler, T. L. Thomson and M. MacFarland, Transport of water through the tropical tropopause, Geophys. Res. Lett., 9, 617-620, 1982.

Kley, D., and E. J. Stone, Measurement of water vapor in the stratosphere by photodissociation with Ly-α (1216 Å) light, Rev. Sci. Instrum., 49, 691-697, 1978.

***Kley, D., J. Russell III, C. Phillips (eds.), A. Gettelman, J. Harries, P. Mote, S. Oltmans, E. Remsberg, K. Rosenlof, C. Schiller, SPARC Assessment of Water Vapour in the Stratosphere and Upper Troposphere, WCRP-113, WMO/TD No. 1043, SPARC Report No. 2, 2000.

***Konopka, P., G. Günther, R. Müller, F. H. Santos, C. Schiller, A. Ulanovsky, H. Schlager, C. M. Volk, S. Viciani, L. Pan, D. S. McKenna, M. Riese, Mixing-driven troposphere to stratosphere transport (TST) across the TTL, Atmos. Chem. Phys., 7, 3285-3308, 2007.

Koop, T., Luo, B. P.; Tsias, A., Peter, T.; Water activity as the determinant for homogeneous ice nucleation in aqueous solutions, Nature, 406, 611-614, 2000.

Korolev, A. and Mazin, I.: Supersaturation of water vapor in clouds, J. Atmos. Sci., 60, 2957–2976, 2003.

Krämer, M., and A. Afchine, Sampling characteristics of inlets operated at low U/U0 ratios: New insights from computational fluid dynamics (CFX) modelling, J. Aerosol Sci., 35, 683-694, doi:10.1016/j.Jaerosci.2003.11.011, 2004.

**Krämer, M., C. Schiller, C. Voigt, H. Schlager, A climatological view on HNO_3 partitioning in cirrus clouds, Quart. J. Roy. Met. Soc., doi: 10.1002/qj.253, 2008.

***Krämer, M., C. Schiller, A. Afchine, R. Bauer, I. Gensch, A. Mangold, S. Schlicht, N. Spelten, N. Sitnikov, S. Borrmann, M. de Reus, and P. Spichtinger, Ice supersaturations and cirrus cloud crystal numbers, Atmos. Chem. Phys., 9, 3505-3522, 2009.

**Law, K. S., F. Fierli, F. Cairo, H. Schlager, S. Borrmann, M. Streibel, E. Real, D. Kunkel, C. Schiller, F. Ravegnani, A. Ulanovsky, F. D'Amato, S. Viciani, C. M. Volk, Air mass origins influencing TTL chemical composition over West Africa during 2006 summer monsoon, Atmos. Chem. Phys., 10, 10753-10770, 2010.

Lelieveld, J., Brühl, C., Jöckel, P., Steil, B., Crutzen, P. J., Fischer, H., Giorgetta, M. A., Hoor, P., Lawrence, M. G., Sausen, R., Tost, H.: Stratospheric dryness: model simulations and satellite observations, Atmos. Chem. Phys., 7, 1313–1332, 2007.

Le Texier, H., S. Solomon, R. R. Garcia, The role of molecular hydrogen and methane oxidation in the water vapour budget of the stratosphere, Q. J. R. Meteorol. Soc., 114, 281-295, 1988.

Liu, C. L., and E. J. Zipser, Global distribution of convection penetrating the tropical tropopause, J. Geophys. Res., 110, D23104, doi:10.1029/2005JD006063, 2005.

**Lumpe, J. R. Bevilacqua, G. Nedoluha, K. Hoppel, C. Randall, J. Russell, C. Schiller, B. Sen, G. Taha, G. Toon, H. Vömel, Validation of Polar Ozone and Aerosol Measurement (POAM) III version 4 stratospheric water vapor, J. Geophys. Res., 111, D11301, doi:10.1029/2005JD006763, 2006.

***Luo, B. P., B., Th. Peter, S. Flueglistaler, H. Wernli, M. Wirth, C. Kiemle, H. Flentje, V. A. Yushkov, V. Khattatov, V. Rudakov, A. Thomas, S. Borrmann, G. Toci, P. Mazzinghi, J. Beuermann, C. Schiller, F. Cairo, G. Di Donfrancesco, A. Adriani, C. M. Volk, J. Strom, K. Noone, V. Mitev, R. A. MacKenzie, K. S. Carslaw, T. Trautmann, V. Santacesaria, and L. Stefanutti, Dehydration potential of ultrathin clouds at the tropical tropopause, Geophys. Res. Lett., Vol. 30, No. 11, 1557, 10.1029/2002GL016737, 2003a.

**Luo, B. P. ,Th. Peter, H. Wernli, S. Flueglistaler, M. Wirth, C. Kiemle, H. Flentje, V. A. Yushkov, V. Khattatov, V. Rudakov, A. Thomas, S. Borrmann, G. Toci, P. Mazzinghi, J. Beuermann, C. Schiller, F. Cairo, G. Di Donfrancesco, A. Adriani, C. M. Volk, J. Strom, K. Noone, V. Mitev, R. A. MacKenzie, K. S. Carslaw, T. Trautmann, V. Santacesaria, and L. Stefanutti, Ultrathin tropical tropopause clouds (UTTCs): II. stabilization mechanism, Atmos. Chem. Phys., 3, 1093-1100, 2003b.

***MacKenzie, A. R,. C. Schiller, A. Adriani, J. Beuermann, F. Cairo, T. Corti, I. Gensch, M. Krämer, C. Kröger, B. Lepouchov, D. Lowe, S. Merkulov, V. Mitev, A. Oulanovsky, Th. Peter, F. Ravegnani, S. Rohs, V. Rudakov, P. Salter, L. Stefanutti, and V. Yushkov, The tropopause and hygropause in the equatorial Indian Ocean during February and March 1999, J. Geophys. Res., 111, No. D18, D18112, doi: 10.1029/2005JD006639, 2006.

Marti, J., and K. Mauersberger, A survey and new measurements of ice vapor pressure at temperatures between 170 and 250 K, Geophys. Res. Lett., 20, 363-366, 1993.

May, R. D., Open-path, near-infrared tunable diode laser spectrometer for atmospheric measurements of H_2O, J. Geophys. Res., 103, 19161–72, 1998.

May, P. T., G. Allen, G. Vaughan, and P. Connolly, Aerosol and thermodynamic effects on tropical cloud systems during TWPICE and ACTIVE, Atmos. Chem. Phys., 9, 15–24, 2009.

McFarquhar, G. M., and A. J. Heymsfield, Parameterization of tropical cirrus ice crystal size distributions and implications for radiative transfer: results from CEPEX, J. Atmos. Sci., 54, 2187-2200, 1997.

McKenna, D. S., P. Konopka, J.-U. Grooß, G. Günther, R. Müller, R. Spang, D. Offermann, Y. Orsolini: A new Chemical Lagrangian Model of the Stratosphere (CLaMS): Part I Formulation of advection and mixing, J. Geophys. Res., 107, 4309, 2002.

*Meyer, J., Vergleich und Charakterisierung stratosphärisch messender in-situ Hygrometer, Diploma Thesis, RWTH Aachen, 2008.

***Meyer, J., C. Schiller, M. Krämer, M. Kübbeler, S.Rohs, N. Spelten, H. Saathoff, V. Ebert, P. Mackrodt, N. Sitnikov, Data quality of the FISH fluorescence hygrometer, Atmos. Meas. Tech., in preparation, 2011.

**Milz, M. T. v. Clarmann, P. Bernath, C. Boone, S. Chauhan, B. Deuber, D. G. Feist, B. Funke, N. Glatthor, U. Grabowski, A. Griesfeller, A. Haefele, M. Höpfner, N. Kämpfer, S. Kellmann, A. Linden, S. Müller, H. Nakajima, H. Oelhaf, E. Remsberg, S. Rohs, J. M. Russell III, C. Schiller, G. P. Stiller, T. Sugita, T. Tanaka, H. Vömel, K. Walker, G. Wetzel, T. Yokota, V. Yushkov, and G. Zhang, Validation of water vapour profiles (version 13) retrieved by the IMK/IAA scientific retrieval processor based on full resolution spectra measured by MIPAS on board Envisat, Atmos. Meas. Tech., 2, 379-399, 2009.

Mote, P. W., K. H. Rosenlof, M. E. McIntyre, E. S. Carr, J. C. Gille, J. R. Holton, J. S. Kinnersley, H. G. Pumphrey, J. M. Russell III and J. W. Watery, An atmospheric tape recorder: The imprint of tropical tropopause temperatures on stratospheric water vapour, J. Geophys. Res., 101, 3989-4006, 1996.

**Müller, S. C., N. Kämpfer, D. G. Feist, A. Haefele, M. Milz, N. Sitnikov, C. Schiller, C. Kiemle, and J. Urban, Validation of stratospheric water vapour measurements from the airborne microwave radiometer AMSOS, Atmos. Chem. Phys., 8, 3169-3183, 2008.

Murphy, D. M. and T. Koop, Review of the vapour pressures of ice and supercooled water for atmospheric applications, Quart. J. Royal Met. Soc, 131, 1539-1565, 2005.

Murray, B. J., T. W. Wilson, S. Dobbie, Z. Cui, S. M. R. K. Al-Jumur, O. Möhler, M. Schnaiter, R. Wagner, S. Benz, M. Niemand, H. Saathoff, V. Ebert, S. Wagner, B. Kärcher, Heterogeneous nucleation of ice particles on glassy aerosols under cirrus conditions, Nature Geoscience, DOI: 10.1038/NGEO817, 2010.

Newell, R. E, S. Gould-Stewart, A stratospheric fountain, J. Atmos. Sci. 38, 2789-2796, 1981.

**Offermann, D., B. Schaeler, M. Riese, M. Langfermann, M. Jarisch, G. Eidmann, C. Schiller, H. G. J. Smit, W. G. Read, Water vapor at the tropopause during the CRISTA 2 mission, J. Geophys. Res., 107, D23, CRI 4.1-18, 10.1029/2001JD000700, 2002.

Ovarlez, J., Gayet, J.-F., Gierens, K., Ström, J., Ovarlez, H., Auriol, F., Busen, R., and Schumann, U.: Water vapour measurements inside cirrus clouds in Northern and Southern hemispheres during INCA, Geophys. Res. Lett., 29, 1813, doi:10.1029/2001GL014440, 2002.

**Palazzi, E., F. Fierli, F. Cairo, C. Cagnazzo, E. Manzini, F. Ravegnani, C. Schiller, F. D'Amato, and C. M. Volk, Diagnostics of the Tropical Tropopause Layer from in-situ observations and CCM data, Atmos. Chem. Phys., 9, 9349-9367, 2009.

**Peter, T., B. P. Luo, H. Wernli, M. Wirth, C. Kiemle, H. Flentje, V. A. Yushkov, V. Khattatov, V. Rudakov, A. Thomas, S. Borrmann, G. Toci, P. Mazzinghi, J. Beuermann, C. Schiller, F. Cairo, G. Di Donfrancesco, A. Adriani, C. M. Volk, J. Strom, K. Noone, V. Mitev, R. A. MacKenzie, K. S. Carslaw, T. Trautmann, V. Santacesaria, and L. Stefanutti, Ultrathin tropical tropopause clouds: I. Cloud morphology and occurrence, Atmos. Chem. Phys., 3, 1083-1091, 2003.

Peter, T., C. Marcolli, P. Spichtinger, T. Corti, M. Baker, T. Koop, When dry air is too humid, Science, 314, 1399-1401, 2006.

Plöger, F., P. Konopka, G. Günther, J.-U. Grooß, and R. Müller, Impact of the vertical velocity scheme on modeling transport in the tropical tropopause layer (TTL), J. Geophys. Res., 115, D3, doi:10.1029/2009JD012023, 2010.

**Plöger, F., S. Fueglistaler, J.-U. Grooß, G. Günther, P. Konopka, S. Liu, R. Müller, E. Ravegnani, C. Schiller, A. Ulanowski, M. Riese, Insight from ozone and water vapor on transport in the tropical tropopause layer, Atmos. Chem. Phys., 11, 407-419, 2011.

Popp, P. J., Marcy, T. P., Watts, L. A., Gao, R. S., Fahey, D. W., Weinstock, E. M., Smith, J. B., Herman, R. L., Troy, R. F., Webster, C., Christensen, L. E., Baumgardner, D. G., Voigt, C., Kärcher, B., Wilson, J. C., Mahoney, M. J., Jensen, E. J., and Bui, T. P., Condensed-phase nitric acid in a tropical subvisible cirrus clouds, Geophys. Res. Lett., 34, L24812, doi:10.1029/2007GL031832, 2007.

Randel, W. J., F. Wu, S. J. Oltmans, K. Rosenlof, G. E. Nedoluha, Interannual Changes of Stratospheric Water Vapor and Correlations with Tropical Tropopause Temperatures, J. Atmos. Sci., 61, 2133-2148, 2004.

Randel, W. J., et al., Decreases in stratospheric water vapor since 2001: links to changes in the tropical tropopause and the Brewer-Dobson circulation, J. Geophys. Res., 111, doi:10.1029/2005JD006744, 2006.

Randel, W. J., and M. Park, Deep convective influence on the Asian monsoon anticyclone and associated tracer variability observed with Atmospheric Infrared Sounder (AIRS), J. Geophys. Res., 111, D12314, doi: 10.1029/2005JD006490, 2006.

**Ren, C., A. R. MacKenzie, C. Schiller, G. Shur, V. Yushkov, Diagnosis of processes controlling water vapour in the tropical tropopause layer by a Lagrangian cirrus model, Atmos. Chem. Phys., 7, 5401-5413, 2007.

**Rohs, S., C. Schiller, A. Engel, U. Schmidt, T. Wetter, I. Levin, T. Nakazawa, S. Aoki, Long-term changes of methane and hydrogen in the stratosphere in the period 1978-2003, J. Geophys. Res., 111, D14315, doi:10.1029/2005JD006877, 2006.

Rosenlof, K. H., S. J. Oltmans, D. Kley, W. J. Russell III, E.-W. Chiou, W. P. Chu, D. G. Johnson, K. K. Kelly, H. A. Michelsen, G. E. Nedoluha, E. E. Remsberg, G. C. Toon, and M. P. McCormick, Stratospheric water vapor increases over the past half-century, Geophys. Res. Lett., 28, 1195-1198, 2001.

**Santacesaria, V., R. Carla', R. MacKenzie, A. Adriani, F. Cairo, G. Didonfrancesco, C. Kiemle, G. Redaelli, J. Beuermann, C. Schiller, T. Peter, B. Luo, H. Wernli, F. Ravegnani, A. Ulanovsky, V. Yushkov, S. Balestri, L. Stefanutti, Clouds at the tropical tropopause: a case study during the APE-THESEO campaign over the western Indian Ocean, J. Geophys. Res., Vol. 108, No. D2, 10.1029/2002JD002166, 2003.

Scherer, M., H. Vömel, S. Fueglistaler, S. J. Oltmans, and J. Staehelin, Trends and variability of midlatitude stratospheric water vapour deduced from the re-evaluated Boulder balloon series and HALOE, Atmos. Chem. Phys., 8, 1391-1402, 2008.

***Schiller, C., Th. Peter, K. H. Rosenlof, SPARC water vapour initiative, SPARC Newsletter, 30, 16, 2008b.

***Schiller, C., M. Krämer, A. Afchine, N. Spelten, N. Sitnikov, The ice water content of Arctic, mid latitude and tropical cirrus, J. Geophys. Res., 113, D24208, doi:10.1029/2008JD010342, 2008.

***Schiller, C., J.-U. Grooß, P. Konopka, F. Plöger, F. H. Silva dos Santos, N. Spelten, Hydration and dehydration at the tropical tropopause, Atmos. Chem. Phys., 9, 9647-9660, 2009.

*Schlicht, S., Untersuchung zur Wasser-Partitionierung in Zirruswolken, Ph.D. thesis Univ. Wuppertal (2006).

Sherwood, S. C., and A. E. Dessler, On the control of stratospheric humidity, Geophys. Res. Lett., 27, 2513-2516, 2000.

*Silva dos Santos F. H., Hydratation und Dehydratation in der tropischen Tropopausenschicht, PhD Thesis Univ. Wuppertal, 2008.

**Sitnikov, N. M., V. A. Yushkov, A. A. Afchine, L. I. Korshunov, V. I. Astakhov, A. E. Ulanovskii, M. Kraemer, A. Mangold, C. Schiller, and F. Ravegnani, The FLASH instrument for water vapor measurements on board the high-altitude airplane, Russian Journal on Instruments and Experimental Techniques, 50, 1, 113-121, 2007.

Solomon, S., The mystery of the Antarctic ozone "hole", Rev. Geophys., 26, 1, doi:10.1029/RG026i001p00131, 1988.

Solomon, S., K. Rosenlof, R. Portman, J. Daniel, S. Davies, T. Sanford, G.-K. Plattner, Contributions of stratospheric water vapor to decadal changes in the rate of global warming, Science, 10.1126/science.1182488, 2010.

Sonntag, D., Advancements in the field of hygrometry, Meteorol. Z., N. F., 3, 51-66, 1994.

Stefanutti, L., L. Sokolov, S. Balestri, A. R. MacKenzie, V. Khattatov, The M-55 Geophysica as a Platform for the Airborne Polar Experiment. Journal of Atmospheric and Oceanic Technology: Vol. 16, No. 10, pp. 1303-1312, 1999.

**Stefanutti, L., A. R. MacKenzie, V. Santacesaria, A. Adriani, S. Balestri, S. Borrmann, V. Khattatov, P. Mazinghi, S. Merkulov, V. Mitev, V. Rudakov, C. Schiller, G. Toci, M. Volk, V. Yushkov, H. Flentje, C. Kiemle, K. Noone, G. Redaelli, K. S. Carslaw, Th. Peter, The APE-THESEO tropical campaign: an overview, J. Atmos. Chem., 48 (1): 1-33, 2004.

Teitelbaum, H., M. Moustaoui, R. Sadourny, F. Lott, Critical levels and mixing layers induced by convectively generated gravity waves during CEPEX, Q. J. R. Meteorol. Soc., 125, 1715–1734, 1999.

Thomason, L. W., J. R. Moore, M. C. Pitts, J. M. Zawodny, and E.W. Chiou, An evaluation of the SAGE III version 4 aerosol extinction coefficient and water vapor data products, Atmos. Chem. Phys., 10, 2159–2173, 2010.

Tost, H., M. G. Lawrence, C. Brühl, P. Jöckel, The GABRIEL Team, The SCOUT-O3-DARWIN/ACTIVE Team, Uncertainties in atmospheric chemistry modelling due to convection parameterisations and subsequent scavenging, Atmos. Chem. Phys., 10, 1931–1951, 2010

***Vaughan, G., C. Schiller, A. R. MacKenzie, K. Bower, T. Peter, H. Schlager, N. R. P. Harris and P. T. May, SCOUT-O3 /ACTIVE: High-altitude aircraft measurements around deep tropical convection, Bull. Amer. Meteorol. Soc., 89, 647-662, doi:10.1175/BAMS-89-5-647, 2008.

**Voigt, C., Schlager, H., Ziereis, H., K¨archer, B., Luo, B.P., Schiller, C., Krämer, M., Irie, H., Kondo Y. and Popp, P.,. Nitric acid uptake in cirrus clouds. Geophys. Res. Lett., 33, L05803, doi:10.1029/2005GL025159, 2006.

**Voigt, C., Kärcher, B., Schlager, H., Schiller, C., Krämer, M., de Reus, M., Vössing, H., Borrmann, S., and Mitev, V.: In-situ observations and modeling of small nitric acid-containing ice crystals, Atmos. Chem. Phys., 7, 3373–3383, 2007.

**Voigt, C., H. Schlager, A. Roiger, A. Stenke, M. de Reus, S. Borrmann, E. Jensen, C. Schiller, P. Konopka, and N. Sitnikov, Detection of reactive nitrogen containing particles in the tropopause region – evidence for a tropical nitric acid trihydrate (NAT) belt, Atmos. Chem. Phys., 8, 7421-7430, 2008.

**von Hobe, M., J.-U. Grooß, G. Günther, P. Konopka, I. Gensch, M. Krämer, N. Spelten, A. Afchine, C. Schiller, A. Ulanovsky, N. Sitnikov, G. Shur, V. Yushkov, F. Ravegnani, F. Cairo, A. Roiger, C. Voigt, H. Schlager, R. Weigel, W. Frey, S. Borrmann, R. Müller, F. Stroh, Evidence for heterogeneous chlorine activation in the tropical UTLS, Atmos. Chem. Phys., 11, 241-256, 2011.

Vömel, H, J. E. Barnes, R. N. Forno, M. Fujiwara, F. Hasebe, S. Iwasaki, R. Kivi, N. Komala, E. Kyrö, T. Leblanc, B. Morel, S.-Y. Ogino, W. G. Read, S. C. Ryan, S. Saraspriya, H. Selkirk, M. Shiotani, J. Valverde Canossa, and D. N. Whiteman, Validation of Aura Microwave Limb Sounder water vapor by balloonborne Cryogenic Frost point Hygrometer measurements, J. Geophys. Res., 112, D24S37, doi:10.1029/2007JD008698, 2007.

Wang, Z., and K. Sassen, Cirrus cloud microphysical property retrieval using lidar and radar measurements. Part II: Midlatitude cirrus microphysical and radiative properties, J. Atmos. Sci., 59, 2291-2303, 2002.

Weinstock, E. M., J. B. Smith, D. S. Sayres, J. V. Pittman, J. R. Spackman, E. J. Hintsa, T. F. Hanisco, E. J. Moyer, J. M. St. Clair, M. R. Sargent, J. G. Anderson, Validation of the Harvard Lyman-α in situ water vaor instrument: Implications for the mechanisms that control stratospheric water vapor, J. Geophys. Res., 114, D23301, doi:10.1029/2009JD012427, 2009.

Zobrist, B., Marcolli, C., Pedernera, D. A. & Koop, T. Do atmospheric aerosols, form glasses? Atmos. Chem. Phys. 8, 5221_5244 (2008).

*Zöger, M., Entwicklung eines flugzeuggetragenen Hygrometers für den Einsatz in der Stratosphäre, PhD Thesis Univ. Köln, 1996.

***Zöger, M., A. Afchine, N. Eicke, M.-T. Gerhards, E. Klein, D. S. McKenna, U. Mörschel, U. Schmidt, V. Tan, F. Tuitjer, T. Woyke, and C. Schiller, Fast in situ stratospheric hygrometers: A new family of balloonborne and airborne Lyman-α photofragment fluorescence hygrometers, J. Geophys. Res., 104, 1807-1816, 1999.

Reprints of key publications

Corti, T., B. P. Luo, M. deReus, D. Brunner, F. Cairo, M. J. Mahoney, G. Matucci, R. Matthey, V. Mitev, F. H. dos Santos, C. Schiller, G. Shur, N. M. Sitnikov, N. Spelten, H. J. Vössing, S. Borrmann, and T. Peter, Unprecedented evidence for overshooting convection hydrating the tropical stratosphere, Geophys. Res. Lett., 35, L10810, doi:10.1029/2008GL033641, 2008.

Konopka, P., G. Günther, R. Müller, F. H. Santos, C. Schiller, A. Ulanovsky, H. Schlager, C. M. Volk, S. Viciani, L. Pan, D. S. McKenna, M. Riese, Mixing-driven troposphere to stratosphere transport (TST) across the TTL, Atmos. Chem. Phys., 7, 3285-3308, 2007.

Krämer, M., C. Schiller, A. Afchine, R. Bauer, I. Gensch, A. Mangold, S. Schlicht, N. Spelten, N. Sitnikov, S. Borrmann, M. de Reus, and P. Spichtinger, Ice supersaturations and cirrus cloud crystal numbers, Atmos. Chem. Phys., 9, 3505-3522, 2009.

Luo, B. P., Th. Peter, S. Flueglistaler, H. Wernli, M. Wirth, C. Kiemle, H. Flentje, V. A. Yushkov, V. Khattatov, V. Rudakov, A. Thomas, S. Borrmann, G. Toci, P. Mazzinghi, J. Beuermann, C. Schiller, F. Cairo, G. Di Donfrancesco, A. Adriani, C. M. Volk, J. Strom, K. Noone, V. Mitev, R. A. MacKenzie, K. S. Carslaw, T. Trautmann, V. Santacesaria, and L. Stefanutti, Dehydration potential of ultrathin clouds at the tropical tropopause, Geophys. Res. Lett., Vol. 30, No. 11, 1557, 10.1029/2002GL016737, 2003a.

MacKenzie, A. R,. C. Schiller, A. Adriani, J. Beuermann, F. Cairo, T. Corti, I. Gensch, M. Krämer, C. Kröger, B. Lepouchov, D. Lowe, S. Merkulov, V. Mitev, A. Oulanovsky, Th. Peter, F. Ravegnani, S. Rohs, V. Rudakov, P. Salter, L. Stefanutti, and V. Yushkov, The tropopause and hygropause in the equatorial Indian Ocean during February and March 1999, J. Geophys. Res., 111, No. D18, D18112, doi: 10.1029/2005JD006639, 2006.

Meyer, J., C. Schiller, M. Krämer, M. Kübbeler, S.Rohs, N. Spelten, H. Saathoff, V. Ebert, P. Mackrodt, N. Sitnikov, Data quality of the FISH fluorescence hygrometer, Atmos. Meas. Tech., in preparation, 2011.

Schiller, C., Th. Peter, K. H. Rosenlof, SPARC water vapour initiative, SPARC Newsletter, 30, 16, 2008b.

Schiller, C., M. Krämer, A. Afchine, N. Spelten, N. Sitnikov, The ice water content of Arctic, mid latitude and tropical cirrus, J. Geophys. Res., 113, D24208, doi:10.1029/2008JD010342, 2008.

Schiller, C., J.-U. Grooß, P. Konopka, F. Plöger, F. H. Silva dos Santos, N. Spelten, Hydration and dehydration at the tropical tropopause, Atmos. Chem. Phys., 9, 9647-9660, 2009.

Vaughan, G., C. Schiller, A. R. MacKenzie, K. Bower, T. Peter, H. Schlager, N. R. P. Harris and P. T. May, SCOUT-O3 /ACTIVE: High-altitude aircraft measurements around deep tropical convection, Bull. Amer. Meteorol. Soc., 89, 647-662, doi:10.1175/BAMS-89-5-647, 2008.

Zöger, M., A. Afchine, N. Eicke, M.-T. Gerhards, E. Klein, D. S. McKenna, U. Mörschel, U. Schmidt, V. Tan, F. Tuitjer, T. Woyke, and C. Schiller, Fast in situ stratospheric hygrometers: A new family of balloonborne and airborne Lyman-α photofragment fluorescence hygrometers, J. Geophys. Res., 104, 1807-1816, 1999.

Not reprinted, available via www.atmosp.physics.utoronto.ca/SPARC/index.html

Kley, D., J. Russell III, C. Phillips (eds.), A. Gettelman, J. Harries, P. Mote, S. Oltmans, E. Remsberg, K. Rosenlof, C. Schiller, SPARC Assessment of Water Vapour in the Stratosphere and Upper Troposphere, WCRP-113, WMO/TD No. 1043, SPARC Report No. 2, 2000.

Unprecedented evidence for deep convection hydrating the tropical stratosphere

T. Corti, B.P. Luo, M. de Reus, D. Brunner, F. Cairo, M.J. Mahoney, G. Martucci, R. Matthey, V. Mitev, F.H. dos Santos, C. Schiller, G. Shur, N.M. Sitnikov, N. Spelten, H.J. Vössing, S. Borrmann, and T. Peter.

We report on in situ and remote sensing measurements of ice particles in the tropical stratosphere found during the Geophysica campaigns TROCCINOX and SCOUT-O3. We show that the deep convective systems penetrated the stratosphere and deposited ice particles at altitudes reaching 420 K potential temperature. These convective events had a hydrating effect on the lower tropical stratosphere due to evaporation of the ice particles. In contrast, there were no signs of convectively induced dehydration in the stratosphere.

Corti, T., et al. (2008), Unprecedented evidence for deep convection hydrating the tropical stratosphere, Geophys. Res. Lett., 35, L10810, doi:10.1029/2008GL033641.

© Copyright 2008 American Geophysical Union (AGU). Reproduced by permission.

Contribution of mixing to upward transport across the tropical tropopause layer (TTL)

P. Konopka, G. Günther, R. Müller, F. H. S. dos Santos, C. Schiller, F. Ravegnani, A. Ulanovsky, H. Schlager, C. M. Volk, S. Viciani, L. L. Pan, D.-S. McKenna, and M. Riese

During the second part of the TROCCINOX campaign that took place in Brazil in early 2005, chemical species were measured on-board the high-altitude research aircraft Geophysica (ozone, water vapor, NO, NO_y, CH_4 and CO) in the altitude range up to 20 km (or up to 450 K potential temperature), i.e. spanning the entire TTL region roughly extending between 350 and 420 K. Here, analysis of transport across the TTL is performed using a new version of the Chemical Lagrangian Model of the Stratosphere (CLaMS). In this new version, the stratospheric model has been extended to the earth surface. Above the tropopause, the isentropic and cross-isentropic advection in CLaMS is driven by meteorological analysis winds and heating/cooling rates derived from a radiation calculation. Below the tropopause, the model smoothly transforms from the isentropic to the hybrid-pressure coordinate and, in this way, takes into account the effect of large-scale convective transport as implemented in the vertical wind of the meteorological analysis. As in previous CLaMS simulations, the irreversible transport, i.e. mixing, is controlled by the local horizontal strain and vertical shear rates. Stratospheric and tropospheric signatures in the TTL can be seen both in the observations and in the model. The composition of air above ≈350 K is mainly controlled by mixing on a time scale of weeks or even months. Based on CLaMS transport studies where mixing can be completely switched off, we deduce that vertical mixing, mainly driven by the vertical shear in the tropical flanks of the subtropical jets and, to some extent, in the the outflow regions of the large-scale convection, offers an explanation for the upward transport of trace species from the main convective outflow at around 350 K up to the tropical tropopause around 380 K.

Konopka, P., et al. (2007), Contribution of mixing to upward transport across the tropical tropopause layer (TTL), Atmos. Chem. Phys., 7, 3285–3308, doi:10.5194/acp-7-3285-2007.

© Authors 2007. This work is licensed under the Creative Commons Attribution-NonCommercial-ShareAlike 2.5 License.

Ice supersaturations and cirrus cloud crystal numbers

M. Krämer, C. Schiller, A. Afchine, R. Bauer, I. Gensch, A. Mangold, S. Schlicht, N. Spelten, N. Sitnikov, S. Borrmann, M. de Reus, and P. Spichtinger

Upper tropospheric observations outside and inside of cirrus clouds indicate water vapour mixing ratios sometimes exceeding water saturation. Relative humidities over ice (RH_{ice}) of up to and more than 200% have been reported from aircraft and balloon measurements in recent years. From these observations a lively discussion continues on whether there is a lack of understanding of ice cloud microphysics or whether the water measurements are tainted with large uncertainties or flaws. Here, RH_{ice} in clear air and in ice clouds is investigated. Strict quality-checked aircraft in situ observations of RH_{ice} were performed during 28 flights in tropical, mid-latitude and Arctic field experiments in the temperature range 183–240 K. In our field measurements, no supersaturations above water saturation are found. Nevertheless, super- or subsaturations inside of cirrus are frequently observed at low temperatures (<205 K) in our field data set. To explain persistent RH_{ice} deviating from saturation, we analysed the number densities of ice crystals recorded during 20 flights. From the combined analysis – using conventional microphysics – of supersaturations and ice crystal numbers, we show that the high, persistent supersaturations observed inside of cirrus can possibly be explained by unexpected, frequent very low ice crystal numbers that could scarcely be caused by homogeneous ice nucleation. Heterogeneous ice formation or the suppression of freezing might better explain the observed ice crystal numbers. Thus, our lack of understanding of the high supersaturations, with implications for the microphysical and radiative properties of cirrus, the vertical redistribution of water and climate, is traced back to the understanding of the freezing process at low temperatures.

Krämer, M., Schiller, C., Afchine, A., Bauer, R., Gensch, I., Mangold, A., Schlicht, S., Spelten, N., Sitnikov, N., Borrmann, S., de Reus, M., and Spichtinger, P. (2009), Ice supersaturations and cirrus cloud crystal numbers, Atmos. Chem. Phys., 9, 3505–3522, doi:10.5194/acp-9-3505-2009.

© Authors 2009. This work is distributed under the Creative Commons Attribution 3.0 License.

Dehydration potential of ultrathin clouds at the tropical tropopause

B. P. Luo, T. Peter, S. Fueglistaler, H. Wernli, M. Wirth, C. Kiemle, H. Flentje, V. A. Yushkov, V. Khattatov, V. Rudakov, A. Thomas, S. Borrmann, G. Toci, P. Mazzinghi, J. Beuermann, C. Schiller, F. Cairo, G. Di Donfrancesco, A. Adriani, C. M. Volk, J. Strom, K. Noone, V. Mitev, R. A. MacKenzie, K. S. Carslaw, T. Trautmann, V. Santacesaria, and L. Stefanutti

We report on the first simultaneous *in situ* and remote measurements of subvisible cirrus in the uppermost tropical troposphere. The observed cirrus, called UTTCs (ultrathin tropical tropopause clouds), are the geometrically (200–300 m) and optically ($\tau \approx 10^{-4}$) thinnest large-scale clouds ever sampled ($\approx 10^5$ km^2). UTTCs consist of only a few ice particles per liter with mean radius ≈5 μm, containing only 1–5 % of the total water. Yet, brief adiabatic cooling events only 1–2 K below mean ambient temperature destabilize UTTCs, leading to large sedimenting particles ($r \approx 25$ μm). Due to their extreme altitude above 17 km and low particle number density, UTTCs may efficiently dehydrate air during its last encounter with the ice phase before entering the stratosphere.

Luo, B. P., et al., (2003), Dehydration potential of ultrathin clouds at the tropical tropopause, Geophys. Res. Lett., 30(11), 1557, doi:10.1029/2002GL016737.

© Copyright 2003 American Geophysical Union (AGU). Reproduced by permission.

Tropopause and hygropause variability over the equatorial Indian Ocean during February and March 1999

A. R. MacKenzie, C. Schiller, T. Peter, A. Adriani, J. Beuermann, O. Bujok, F. Cairo, T. Corti, G. DiDonfrancesco, I. Gensch, C. Kiemle, M. Krämer, C. Kröger, S. Merkulov, A. Oulanovsky, F. Ravegnani, S. Rohs, V. Rudakov, P. Salter, V. Santacesaria, L. Stefanutti, and V. Yushkov

Measurements of temperature, water vapor, total water, ozone, and cloud properties were made above the western equatorial Indian Ocean in February and March 1999. The cold-point tropopause was at a mean pressure-altitude of 17 km, equivalent to a potential temperature of 380 K, and had a mean temperature of 190 K. Total water mixing ratios at the hygropause varied between 1.4 and 4.1 ppmv. The mean saturation water vapor mixing ratio at the cold point was 3.0 ppmv. This does not accurately represent the mean of the measured total water mixing ratios because the air was unsaturated at the cold point for about 40% of the measurements. As well as unsaturation at the cold point, saturation was observed above the cold point on almost 30% of the profiles. In such profiles the air was saturated with respect to water ice but was free of clouds (i.e., backscatter ratio <2) at potential temperatures more than 5 K above the tropopause and hygropause. Individual profiles show a great deal of variability in the potential temperatures of the cold point and hygropause. We attribute this to short timescale and space-scale perturbations superimposed on the seasonal cycle. There is neither a clear and consistent “setting” of the tropopause and hygropause to the same altitude by dehydration processes nor a clear and consistent separation of tropopause and hygropause by the Brewer-Dobson circulation. Similarly, neither the tropopause nor the hygropause provides a location where conditions consistently approach those implied by a simple “tropopause freeze drying” or “stratospheric fountain” hypothesis.

MacKenzie, A. R., et al. (2006), Tropopause and hygropause variability over the equatorial Indian Ocean during February and March 1999, J. Geophys. Res., 111, D18112, doi:10.1029/2005JD006639.

© Copyright 2006 American Geophysical Union (AGU). Reproduced by permission.

Two decades of water vapor measurements with the FISH fluorescence hygrometer: a review

J. Meyer, C. Rolf, C. Schiller, S. Rohs, N. Spelten, A. Afchine, M. Zöger, N. Sitnikov, T. D. Thornberry, A. W. Rollins, Z. Bozóki, D. Tátrai, V. Ebert, B. Kühnreich, P. Mackrodt, O. Möhler, H. Saathoff, K. H. Rosenlof, and M. Krämer

For almost two decades, the airborne Fast In-situ Stratospheric Hygrometer (FISH) has stood for accurate and precise measurements of total water mixing ratios (WMR, gas phase + evaporated ice) in the upper troposphere and lower stratosphere (UT/LS). Here, we present a comprehensive review of the measurement technique (Lyman-α photofragment fluorescence), calibration procedure, accuracy and reliability of FISH. Crucial for FISH measurement quality is the regular calibration to a water vapor reference, namely the commercial frost-point hygrometer DP30. In the frame of this work this frost-point hygrometer is compared to German and British traceable metrological water standards and its accuracy is found to be 2–4 %. Overall, in the range from 4 to 1000 ppmv, the total accuracy of FISH was found to be 6–8 %, as stated in previous publications. For lower mixing ratios down to 1 ppmv, the uncertainty reaches a lower limit of 0.3 ppmv. For specific, non-atmospheric conditions, as set in experiments at the AIDA chamber – namely mixing ratios below 10 and above 100 ppmv in combination with high- and low-pressure conditions – the need to apply a modified FISH calibration evaluation has been identified. The new evaluation improves the agreement of FISH with other hygrometers to ± 10 % accuracy in the respective mixing ratio ranges. Furthermore, a quality check procedure for high total water measurements in cirrus clouds at high pressures (400–500 hPa) is introduced. The performance of FISH in the field is assessed by reviewing intercomparisons of FISH water vapor data with other in situ and remote sensing hygrometers over the last two decades. We find that the agreement of FISH with the other hygrometers has improved over that time span from overall up to ± 30 % or more to about ± 5–20 % @ < 10 ppmv and to ± 0–15 % @ > 10 ppmv. As presented here, the robust and continuous calibration and operation procedures of the FISH instrument over the last two decades establish the position of FISH as one of the core instruments for in situ observations of water vapor in the UT/LS.

Meyer, J., Rolf, C., Schiller, C., Rohs, S., Spelten, N., Afchine, A., Zöger, M., Sitnikov, N., Thornberry, T. D., Rollins, A. W., Bozóki, Z., Tátrai, D., Ebert, V., Kühnreich, B., Mackrodt, P., Möhler, O., Saathoff, H., Rosenlof, K. H., and Krämer, M. (2015) Two decades of water vapor measurements with the FISH fluorescence hygrometer: a review, Atmos. Chem. Phys., 15, 8521-8538, doi:10.5194/acp-15-8521–2015.

(*This paper was included in the thesis as a draft and has now appeared in Atmos. Chem. Phys.)*

© Authors 2015. This work is distributed under the Creative Commons Attribution 3.0 License.

SPARC Water Vapour Initiative

C. Schiller, Forschungszentrum Jülich, Germany (c.schiller@fz-juelich.de)
T. Peter, ETH Zürich, Switzerland (thomas.peter@env.ethz.ch)
K. Rosenlof, NOAA, USA (Karen.H.Rosenlof@noaa.gov)

In the year 2000, SPARC published its Assessment of Upper Tropospheric and Stratospheric (UTS) Water Vapour (SPARC Report No. 2, WCRP-113, WMO/TD No. 1043), which was coordinated and edited by Dieter Kley, Jim M. Russell III and Celine Phillips. The key topic addressed in this report was the analysis and the assessment of the long-term changes of UTS water vapour, with an emphasis on the observed increase of water in the stratosphere. The report had a strong focus describing and comparing relevant data sets using *in situ* hygrometers and remote sensing instruments from laboratories all over the world in order to create a suitable data set, including historical data back to the 1940s. Data presented is the report are available at the SPARC data centre at **http://www.sparc.sunysb.edu/**. The distribution and variability of UTS water vapour, the relevant processes, and the impact of the increased water vapour on radiation, dynamics and chemistry were discussed. However, a quantitative explanation of the analysed changes was not possible in 2000.

Following the recommendations of this report, climatological measurement programmes have continued, new campaigns to investigate UTS water vapour have been carried out, new satellite observation programmes have been launched, and many model and laboratory studies have been made since 2000 to explain the observations and to identify previously unknown processes. Emerging from the new observations, an additional "puzzling" question became apparent in that unexpected high relative humidities were observed, largely in the cold tropopause region both inside and outside of clouds (see contribution by Peter, Krämer and Möhler, this issue). Data quality, in particular knowing the absolute accuracy and not simply the relative discrepancies between different sensors, has become a crucial issue if we are to assess these questions. These accuracy issues have lead to the need of cross validation of established and recently developed hygrometers, both in the field and in the laboratory.

In light of these developments, it seems timely to update the SPARC water vapour assessment of 2000. In particular, there is a need to summarise the relevant results over the past decade from various field experiments, laboratories and models in a comprehensive report or review publication. The major goal of such an exercise is to assess the value and the accuracy of recent measurements and to give new recommendations and guidelines for future research on UTS water vapour. The major topics to be addressed are:

1. **Data quality:** How reliable are *in situ* and remote sensing field data in terms of accuracy and precision?
2. **Clear air and in-cloud supersaturation:** Can the observations be explained within the framework of our current knowledge or do we need new theoretical concepts and new laboratory investigations, *e.g.* of ice growth at extreme temperatures?
3. **Recent observations of UTS water vapour changes:** Are these observations mutually consistent, do we understand them, and what are our abilities for future predictions?
4. **Impact on atmospheric chemistry and climate:** What are the implications of changing UTS water vapour for radiation, dynamics, chemistry, clouds and climate?

Therefore, the SPARC Scientific Steering Group proposed during its annual meeting in September 2007 to initiate a new water vapour initiative, which will be coordinated by Cornelius Schiller, Thomas Peter and Karen Rosenlof. A kick-off workshop for the community will be organised in 2008, preferably connected to the SPARC General Assembly in Bologna (August 31 – September 5, 2008). More detailed information will be provided soon to the community concerned with water vapour issues.

Ice water content of Arctic, midlatitude, and tropical cirrus

C. Schiller, M. Krämer, A. Afchine, N. Spelten, N. Sitnikov

In situ measurements of total water have been obtained during several airborne field experiments in the Arctic (POLSTAR 1997 and 1998; EUPLEX/ENVISAT 2003), at midlatitudes (ENVISAT 2002, Cirrus 2003 and 2004, TROCCINOX 2005), and in the tropics (APE-THESEO 1999, TROCCINOX/ENVISAT 2005, SCOUT-O3 2005) in 52 flights in cirrus using the Jülich Lyman-α fluorescence hygrometer FISH. For a subset of 28 flights, the measurements are complemented by gas phase measurements of H_2O. From the data set obtained in these experiments, the ice water content (IWC) in cirrus clouds is derived using two different approaches and functions of the minimum, mean, median, and maximum IWC are provided. The data are analyzed as a function of temperature in the range 183–250 K for Arctic, midlatitudinal, and tropical regions thus extending previous climatologies to much lower temperatures and lower detectable IWC. For each temperature, IWC covers a broad band, decreasing with temperature over the whole temperature range. In the tropics, several events of enhanced ice water content are observed which are related to recent impact of convection.

Schiller, C., M. Krämer, A. Afchine, N. Spelten, and N. Sitnikov (2008), Ice water content of Arctic, midlatitude, and tropical cirrus, J. Geophys. Res., 113, D24208, doi:10.1029/2008JD010342.

© Copyright 2008 American Geophysical Union (AGU). Reproduced by permission.

Hydration and dehydration at the tropical tropopause

C. Schiller, J.-U. Grooß, P. Konopka, F. Plöger, F. H. Silva dos Santos, and N. Spelten

High-resolution water measurements from three tropical airborne missions in Northern Australia, Southern Brazil and West Africa in different seasons are analysed to study the transport and transformation of water in the tropical tropopause layer (TTL) and its impact on the stratosphere. The mean profiles are quite different according to the season and location of the campaigns, with lowest mixing ratios below 2 ppmv at the cold point tropopause during the Australian mission in November/December and high TTL mixing ratios during the African measurements in August. We present backward trajectory calculations considering freeze-drying of the air to the minimum saturation mixing ratio and initialised with climatological satellite data. This trajectory-based reconstruction of water agrees well with the observed H_2O average profiles and therefore demonstrates that the water vapour set point in the TTL is primarily determined by the Lagrangian saturation history. Deep convection was found to moisten the TTL, in several events even above the cold point up to 420 K potential temperatures. However, our study does not provide evidence for a larger impact of these highly-localised events on global scales.

Schiller, C., Grooß, J.-U., Konopka, P., Plöger, F., Silva dos Santos, F. H., and Spelten, N. (2009), Hydration and dehydration at the tropical tropopause, Atmos. Chem. Phys., 9, 9647–9660, doi:10.5194/acp-9-9647-2009.

© Authors 2009. This work is distributed under the Creative Commons Attribution 3.0 License.

SCOUT-O3/ACTIVE: High-altitude Aircraft Measurements around Deep Tropical Convection

G. Vaughan, K. Bower, C. Schiller, A. R. MacKenzie, T. Peter, H. Schlager, N. R. P. Harris, and P. T. May

During November and December 2005, two consortia of mainly European groups conducted an aircraft campaign in Darwin, Australia, to measure the composition of the tropical upper-troposphere and tropopause regions, between 12 and 20 km, in order to investigate the transport and transformation in deep convection of water vapor, aerosols, and trace chemicals. The campaign used two high-altitude aircraft—the Russian M55 Geophysica and the Australian Grob 520 Egrett, which can reach 20 and 15 km, respectively—complemented by upward-pointing lidar measurements from the DLR Falcon and low-level aerosol and chemical measurements from the U.K. Dornier-228. The meteorology during the campaign was characterized mainly by premonsoon conditions—isolated afternoon thunderstorms with more organized convective systems in the evening and overnight. At the beginning of November pronounced pollution resulting from widespread biomass burning was measured by the Dornier, giving way gradually to cleaner conditions by December, thus affording the opportunity to study the influence of aerosols on convection. The Egrett was used mainly to sample in and around the outflow from isolated thunderstorms, with a couple of survey missions near the end. The Geophysica–Falcon pair spent about 40% of their flight hours on survey legs, prioritizing remote sensing of water vapor, cirrus, and trace gases, and the remainder on close encounters with storm systems, prioritizing in situ measurements. Two joint missions with all four aircraft were conducted: on 16 November, during the polluted period, sampling a detached anvil from a single-cell storm, and on 30 November, around a much larger multicellular storm.

G. Vaughan, K. Bower, C. Schiller, A. R. MacKenzie, T. Peter, H. Schlager, N. R. P. Harris, and P. T. May (2008), SCOUT-O3/ACTIVE: High-altitude aircraft measurements around deep tropical convection. Bull. Amer. Meteor. Soc., 89, 647–662.

© Copyright 2008 American Meteorological Society (AMS). Used with permission.

Fast in situ stratospheric hygrometers: A new family of balloon-borne and airborne Lyman α photofragment fluorescence hygrometers

M. Zöger, A. Afchine, N. Eicke, M.-T. Gerhards, E. Klein, D.S. McKenna, U. Mörschel, U. Schmidt, V. Tan, F. Tuitjer, T. Woyke, and Cornelius Schiller

A new set of hygrometers based on the Lyman α photofragment fluorescence technique has been developed for operation on aircraft and balloons in the stratosphere and upper troposphere. They combine technical details from existing fluorescence hygrometers with several improvements in order to achieve the highest data quality and to minimize maintenance and operational procedures. With these instruments, stratospheric H_2O measurements can be accomplished with a precision of < 0.2 ppmv at 1 s integration time, as has been demonstrated both in the laboratory and under field deployment. The design enables a rapid exchange of the air sample of the order of 1 s for fast measurements of small-scale variations of the H_2O mixing ratio in the atmosphere. The hygrometer is calibrated using a laboratory calibration bench with approximately 4% accuracy. Measurements made by the hygrometer are compared with a frost point hygrometer during an aircraft mission at H_2O mixing ratios from 280 to 8 ppmv, yielding an agreement between both techniques within the instrumental errors.

Zöger, M., et al. (1999), Fast in situ hygrometers: A new family of balloonborne and airborne Lyman-α photofragment fluorescence hygrometers, J. Geophys. Res., 104, 1807–1816.

© Copyright 1999 American Geophysical Union (AGU). Reproduced by permission.

Band / Volume 282
Modelling and Experimental Validation of the Viscosity of Liquid Phases in Oxide Systems Relevant to Fuel Slags
G. Wu (2015), XVI, 170 pp
ISBN: 978-3-95806-081-4

Band / Volume 283
Entwicklung von geträgerten protonenleitenden Dünnschichtmembranen für die Wasserstoffabtrennung
W. Deibert (2015), XI, 117 pp
ISBN: 978-3-95806-082-1

Band / Volume 284
Thermochemische Beständigkeit von keramischen Membranen und Katalysatoren für die H_2-Abtrennung in CO-Shift-Reaktoren
E. M. H. Forster (2015), X, 137 pp
ISBN: 978-3-95806-084-5

Band / Volume 285
Spektrale aktinische Flussdichten und Photolysefrequenzen - Untersuchungen in der atmosphärischen Grenzschicht und der freien Troposphäre
I. M. Lohse (2015), VI, 111, VII-XXIII pp
ISBN: 978-3-95806-086-9

Band / Volume 286
Neue Charakterisierungsmethoden für die Gasdiffusionslage in PEM-Brennstoffzellen vor dem Hintergrund produktionsprozessbedingter Materialschwankungen
S. M. Bach (2015), VIII, 149 pp
ISBN: 978-3-95806-088-3

Band / Volume 287
Using the anisotropy of electrical properties for the characterization of sedimentological structures and preferential flow processes
S. Al-Hazaimay (2015), xxii, 94 pp
ISBN: 978-3-95806-090-6

Band / Volume 288
Aktivitätsuntersuchungen und Methoden zur Regeneration von Katalysatoren für die autotherme Reformierung von Dieselkraftstoffen
K. Löhken (2015), II, 147 pp
ISBN: 978-3-95806-093-7

Band / Volume 289
Large-Scale Three Dimensional Modelling of a Direct Methanol Fuel Cell Stack
J. W. McIntyre (2015), 138 pp
ISBN: 978-3-95806-094-4

Band / Volume 290
Abscheidung von Wärmedämmschichtsystemen mit dem Plasma Spray-Physical Vapor Deposition- (PS-PVD-) Prozess – Untersuchung des Prozesses und der hergestellten Schichten
S. Rezanka (2015), XII, 234 pp
ISBN: 978-3-95806-095-1

Band / Volume 291
Characterization & Modification of Copper and Iron Oxide Nanoparticles for Application as Absorber Material in Silicon based Thin Film Solar Cells
M. R. Nuys (2015), XII, 123 pp
ISBN: 978-3-95806-096-8

Band / Volume 292
Interpretation of L-band brightness temperatures of differently tilled bare soil plots
M. Dimitrov (2015), XIV, 116 pp
ISBN: 978-3-95806-098-2

Band / Volume 293
Atrazine in the environment 20 years after its ban: long-term monitoring of a shallow aquifer (in western Germany) and soil residue analysis
D. S. Vonberg (2015), 149 pp
ISBN: 978-3-95806-099-9

Band / Volume 294
Yttria-Stabilized Zirconia / Gadolinium Zirconate Double-Layer Plasma-Sprayed Thermal Barrier Coating Systems (TBCs)
E. Bakan (2015), viii, 131 pp
ISBN: 978-3-95806-100-2

Band / Volume 295
Hydration and dehydration at the tropical tropopause
C. Schiller (2015), 74 pp
ISBN: 978-3-95806-101-9

Weitere ***Schriften des Verlags im Forschungszentrum Jülich*** unter
http://wwwzb1.fz-juelich.de/verlagextern1/index.asp

Energie & Umwelt /
Energy & Environment
Band / Volume 295
ISBN 978-3-95806-101-9